EXPERIMENTAL NEUTRON FLUX MEASUREMENTS AND POWER CALIBRATION IN THE KANSAS STATE UNIVERSITY TRIGA MARK II NUCLEAR REACTOR

by

GARY DON BOUCHEY

B. S., Kansas State University, 1966

A MASTER'S THESIS

submitted in partial fulfillment of the

requirements for the degree

MASTER OF SCIENCE

DEPARTMENT OF NUCLEAR ENGINEERING

KANSAS STATE UNIVERSITY
Manhattan, Kansas

1967

Approved by:

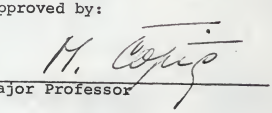

Major Professor

TABLE OF CONTENTS

LIST OF TABLES

LIST OF FIGURES

INTRODUCTION

Knowledge of the neutron intensity in the core is needed in many applications connected with the operation and utilization of a nuclear reactor. This intensity is defined in terms of the neutron flux and expressed in units of neutrons per squared centimeters per second. Much has been written describing the design and the capabilities of the TRIGA Mark II reactor (26, 29, 30), but very few results have been published describing in detail the experimentally measured neutron flux distribution in the TRIGA core. G. B. West (31) of General Atomics has performed multigroup calculations of the neutron flux in the homogenized, uniform core. These calculations, however, frequently do not provide adequate information, hence it is desirable to measure experimentally the flux in the reactor core. Experimental verification of these calculated values are particularly needed for irradiation facilities such as the central thimble and the rotary specimen rack.

Measurement of the neutron flux distribution and calculation of the reactor power level by the integrated flux method in the Kansas State TRIGA core was suggested by W. R. Kimel, head of the Nuclear Engineering Department at Kansas State. Work on this project was first performed by Robert Ihde using indium foils as neutron activation detectors. The results of his work are available in the form of an incompleted Master's thesis entitled Neutron Flux Measurements and Power Calibration in the Kansas State University TRIGA Mark II Nuclear Reactor. Special

credit must be given to Mr. Ihde for his efforts in procuring the Reuter-Stokes miniature fission chamber used for the flux scanning in my work, and for his many helpful suggestions.

This work attempts to provide for the user of the Kansas State University TRIGA Mark II reactor (17) experimental data about the neutron flux useful for planning and performing experiments in the TRIGA core. The specific objective of the work is twofold: first, to determine experimentally the neutron distribution in the Kansas State TRIGA Mark II reactor core and associated irradiation facilities; second, to estimate the reactor power level using the measured distribution in the core. For neutron activation experiments it is convenient to express neutron flux by "Westcott convention" (32) (defined as the neutron density times the velocity of 2200 meters per second). Neutron flux defined in this manner, together with the absorption cross section evaluated at 2200 meters per second, gives for a 1/v absorber the correct absorption rate regardless of the energy distribution of neutrons. Occasionally, for activation of resonance detectors or fast neutron threshold detectors, additional information is needed about the neutron velocity distribution in the core. Values are therefore established for thermal, resonance, and fast fluxes in two of the most frequently used irradiation facilities, the central thimble and the rotary specimen rack.

For measurement of the absolute neutron flux in the TRIGA, standard neutron activation techniques (18, 22) were used. The

determination of an absolute flux is in general difficult; therefore, it was decided to measure the flux carefully at a single point and use this point as the reference for all other flux measurements. For convenience in defining flux, the point should be in a region of well thermalized flux. Such a point is available in the thermal column of the TRIGA reactor. It is hoped that calibration of flux in the thermal column will be useful not only in this work, but as a standard flux value for future experiments at Kansas State. Two independent methods were employed to obtain the absolute activity of foils irradiated at the calibration point in the thermal column. The first method, beta-gamma coincidence, is well known and has been reviewed by several authors (3, 12, 24). The second, the "sum peak" method, is a relatively new and promising technique developed at the Institute for Nuclear Physics Research in the Netherlands (5, 6, 7, 8).

Neutron activation methods developed in the literature (13, 22, 27, 28) are also used for measuring thermal, resonance, and fast flux values for the central thimble and the rotary specimen rack. Since neutron activation is generally a complex and time consuming method, it is difficult to get results for a large number of points. Thus, for the purpose of a detailed scanning of the neutron flux in the core a simple, compact method is desirable. The method selected utilizes a miniature fission chamber capable of operating over large ranges of neutron flux with a high degree of spatial resolution (1, 4, 25).

The total power generated in the core of the TRIGA may be

calculated from the flux plots obtained with the fission chamber. This approach for calculating the power output, called the "integrated flux" method (21, 22), is simple in principle; but it is complicated considerably by the perturbations introduced as a result of the partially inserted control rods and by the heterogeneous nature of the TRIGA core.

Section (1.0) deals with neutron flux measurements in the reactor core and associated irradiation facilities. It is divided into three parts. The first is the absolute thermal flux measurement at the selected point in the thermal column. The second is the measurement of thermal, resonance, and fast fluxes in the central thimble and the rotary specimen rack. The third is the flux scanning with the miniature fission chamber. Section (2.0) presents the reactor power level calculations using the flux measurements taken in Section (1.0). The concluding section summarizes the results of Sections (1.0) and (2.0).

(1.0) Measurement of Neutron Flux in the Reactor Core and Irradiation Facilities

For all irradiations and flux measurement in the Kansas State TRIGA Mark II core and irradiation facilities, Power Level Channel No. 1 on the reactor console was used as the reactor power level indicator. This channel consists of a compensated ion chamber that feeds a multi-range linear recorder coupled with an automatic controlling device for maintaining the selected power level within ± 1% for any one experiment (17). Reactor power levels from day to day are not this reproducible. Experience with the miniature fission chamber and a BF_3 ion chamber introduced in the central thimble indicates that standard deviation between identical power levels over relatively short periods (i.e., about two weeks) is from ± 4% to ± 5%. This compares to a value of ± 3% quoted by General Atomics in the TRIGA Operations and Maintenance Manual (29).

Throughout this work "Westcott convention" (32) has been used to define neutron flux. In this definition flux is written as $\phi = nv_o$ where the quantity n is the total neutron density measured by the neutron detectors, and the velocity v_o is the most probable speed in a Maxwellian distribution at a temperature of 293^oK (2200 meters per second). This method of defining neutron flux is particularly useful in experiments requiring the calculation of reaction rates because it eliminates the necessity of knowing the mean velocity of neutrons in the core and because for a 1/v absorber it allows the use of the cross section at 2200 meters per second.

(1.1) Measurement of Absolute Neutron Flux in the Thermal Column

It would be difficult to measure neutron flux in absolute units at every position required in these experiments. An alternative is to measure the absolute flux at a selected calibration point and use this standardized flux as the reference for other flux measurements. It is important to choose the calibration point at a position where the velocity distribution of neutrons is known. Since "Westcott convention" is used to define flux, the calibration point should be in a region of well thermalized flux so that the contribution to the induced activity from resonance neutrons is small. A point which is accessible and which satisfies the above requirements is provided in the TRIGA thermal column. (See Fig. 1)

All irradiations in the thermal column were performed at an indicated power level of 10 kilowatts in the one inch by one-quarter inch irradiation groove located closest to the center of the column. The groove is located two inches above the horizontal centerline, four inches right of the vertical centerline, and extends three feet eight inches into the column. The foils were positioned four inches from the inner end of the groove with a wooden stringer normally used as a foil holder in the KSU subcritical graphite pile. For detailed drawings of the TRIGA thermal column refer to the TRIGA Operation and Maintenance Manual (29).

The irradiation procedure in the thermal column is further complicated by high radiation levels in the reactor bay if the

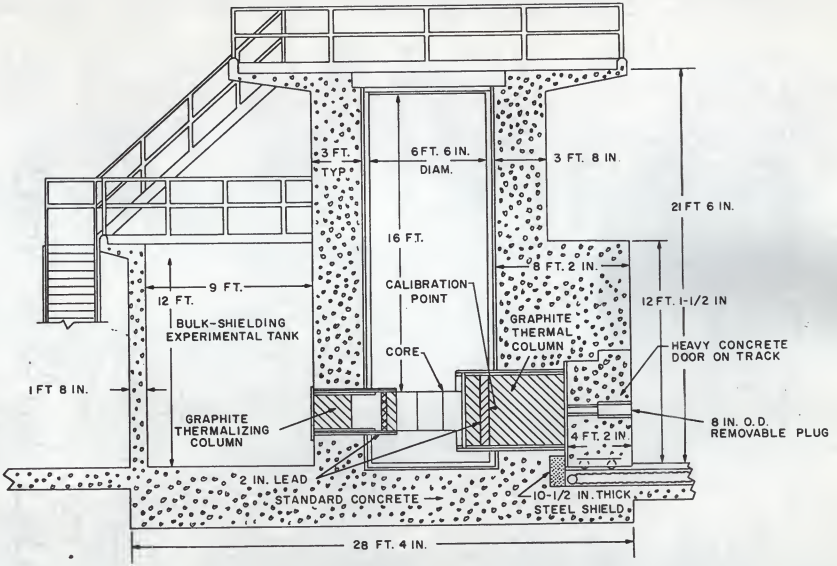

Figure 1. Elevation view of TRIGA Mark II reactor.

thermal column door is open at a power of 10 kilowatts (20). Therefore for each irradiation the sample was inserted and the thermal column door closed before reactor start-up. The reactor was then brought to a power of 10 kilowatts on a period of less than 15 seconds. Timing began the instant the 10 kilowatt level was reached. The maximum additional activity introduced by this procedure for a 15 minute irradiation is approximately 0.05% of the total activity.

By measuring the absolute initial activity of a suitable neutron activation detector irradiated in the thermal column, neutron flux can be calculated from the expression (16)

$$A_o = V\Sigma_a\bar{\phi}(1-e^{-\lambda t}), \qquad (1)$$

where

V = the volume of the irradiated detector,

Σ_a = the macroscopic activation cross section of the detector isotope,

$\bar{\phi}$ = the average neutron flux in the detector,

λ = the radioactive decay constant of the detector isotope, and

t = the irradiation time.

Absolute activities are determined at the selected position using two techniques described in Sections (1.1-a) and (1.1-b).

(1.1-a) Beta-Gamma Coincidence Method for Measuring the Activity of Gold

For the beta-gamma coincidence technique a neutron activation detector that emits a beta-ray in coincidence with a gamma-

ray is irradiated in the thermal column. After irradiation this isotope, decaying at the rate of A disentegrations per second, is counted with two detectors, one that is beta sensitive and one that is gamma sensitive. The count rates obtained are

$$n_\beta = A\varepsilon_\beta \tag{2}$$

where

n_β = the count rate of the beta sensitive detector and

ε_β = the efficiency of the beta detector for beta radiation,

and

$$n_\gamma = A\varepsilon_\gamma \tag{3}$$

where

n_γ = the count rate of the gamma sensitive detector and

ε_γ = the efficiency of the gamma detector for gamma radiation.

The chance of observing a count rate in both detectors simultaneously is given by $\varepsilon_\beta\varepsilon_\gamma$ and the true coincidence count rate $n_{\beta\gamma}$ is given by

$$n_{\beta\gamma} = A\varepsilon_\beta\varepsilon_\gamma. \tag{4}$$

By combining equations (2), (3), and (4), the following expression for absolute activity is obtained:

$$A = \frac{n_\beta n_\gamma}{n_{\beta\gamma}}. \tag{5}$$

In practice the ideal conditions above are difficult to satisfy; thus to get good results from the beta-gamma coincidence method, it is necessary to apply various correction factors (9, 24) to equation (5). For the particular coincidence arrangement used here the only corrections considered were for random (accidental, chance) coincidences and for background coincidences. If $n^*_{\beta\gamma}$ is the total observed coincidence rate, if n_r is the random coincidence count rate due to finite resolving time of the coincidence circuit, and if n_b is the background coincidence rate resulting from cosmic coincidences, then the true count rate can be written as $n_{\beta\gamma} = n^*_{\beta\gamma} - n_r - n_b$.

For two completely independent count rates (n_1 and n_2) obtained from low efficiency detectors, the random count rate is given by $n_r = 2\tau n_1 n_2$ where τ is the resolving time of the coincidence circuit.

A gold foil one mil thick and one-half inch in diameter was used as the neutron detector for the coincidence determination. Gold was selected for two reasons: first, the decay scheme of gold (24) is such that the beta-gamma method applies; second, the activation cross section and other necessary material constants are well established.

The block diagram in Fig. 2 gives the particular arrangement used in the coincidence counting of gold performed for this work. The gamma detector shown is a three inch by three inch NaI(Tl) crystal and the beta detector is a one inch by one-quarter inch plastic scintillation crystal. The Tektronix oscillo-

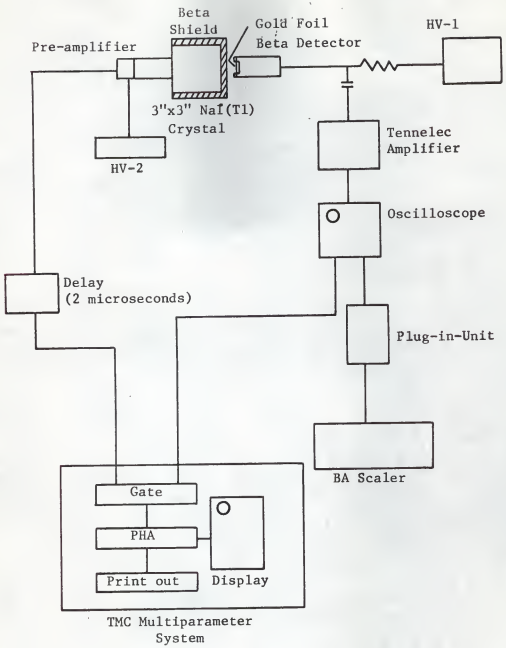

Figure 2. Block diagram of beta-gamma coincidence system.

Equipment: HV-1 John Fluke Power Supply Model 40080A, NE-179, 1300 volts.
HV-2 Fluke HV Power Supply Model 412B, NE-1198, 900 volts.
Tennelec TC 200 Amplifier.
Tektronix Type 545 Oscilloscope, NE-284.
Tektronix Type 53/54L Plug-in-Unit, NE-0284.
Baird Atomic Scaler, NE-145.
Beta Detector - 1"x1/4" Plastic Scintillation Crystal, NE-100.
Gamma Detector - 3"x3" NaI(Tl) Crystal.
TMC 4096 Multiparameter System.

scope in the coincidence system was used as a beta pulse discriminator and shaper. The Tektronix plug-in-unit merely inverts the pulses so they can be accepted by the scaler. The coincidence gating circuit provided in the TMC 4096 multiparameter system may be operated in either the coincidence or anticoincidence mode. The gating pulse provided by the beta detector must have a positive voltage between three and twelve volts, and it must precede the gamma pulse by 250 nanoseconds. Amplification and shaping delays the beta pulse making it necessary to introduce a delay line in the gamma branch of the circuit. Proper adjustment of the delay allows the beta pulses to precede the gamma pulses by the specified time interval.

For each activity determination two counting periods are necessary, one with the gating circuit in the coincidence mode of operation and the other with the gating circuit in the anticoincidence mode. Checking the coincidence and anticoincidence count rates for each determination affords greater confidence in the correct performance of the equipment.

By disregarding background and random coincidences, the fractional standard deviation on A as derived by Campion and Taylor (10) is

$$\sigma_A = \left[\frac{1}{n_{\beta\gamma}} (2\epsilon_\beta\epsilon_\gamma - \epsilon_\beta - \epsilon_\gamma + 1)\right]^{\frac{1}{2}} . \qquad (6)$$

Data taken for the gold foil irradiated for 15 minutes in the thermal column are summarized in Table I. Background has been subtracted from all count rates.

Table I

Beta-Gamma Coincidence of Gold

Time After Removal (hours)	n_γ (c/5 min.)	n_β (c/5 min.)	$n_{\beta\gamma}$ (c/5 min.)	$n_{anticoinc.}$ (c/5 min.)	A (dps)	σ_A (dps)
261.26	201,965	54,695	11,647	190,391	3,161	±57
355.52	71,942	22,463	4,744	67,160	1,135	±32
409.85	41,298	13,945	2,723	37,670	701	±26

For the above case the number of random coincidences is negligible compared to the statistical deviation in the coincidence count rate. Initial activity A_o is calculated from the activity data using the weighted least squares extrapolation program (Appendix A-1) with corrections for using the standard deviations from Table I. The value of initial activity A_o is corrected for flux depression in the vicinity of the foil using the expressions given in the Handbuch der Physik (2). The flux depression factor calculated for a one mil, one-half inch gold foil in a graphite medium is 1.0032. The cadmium ratio at the calibration point is 79.5, making the contribution to the activity from the resonance flux region negligibly small.

The corrected value for initial saturated activity of the gold foil is $(2.60 \pm 0.07) \times 10^4$ dps/gm-watt. By using this initial activity and 98.7 ± 0.6 barns as the activation cross section of gold, the thermal neutron flux at the selected calibration point in the thermal column is $(8.80 \pm 0.25) \times 10^4$ n/cm^2-sec-watt.

(1.1-b) The "Sum Peak" Method for Determining the Activity of Scandium

In the past few years a group from the Institute for Nuclear Physics Research in Amsterdam, Holland has developed a means of determining the absolute activity of a radioactive source which they call the "sum peak" method. In this method, an isotope emitting two gamma-rays in coincidence, each 100% abundant, is counted using a scintillation crystal and a multichannel analyzer. A typical gamma energy spectrum for this case is shown in Fig. 3.

In this figure, A_1 and A_2 denote the areas under the two photopeaks, A_{12} is the area under the sum peak, and T is the total area under the spectrum. Now, defining the photoelectric efficiencies e_1 and e_2 as the probabilities that a gamma-ray is captured in the crystal by a photoelectric process, the total efficiencies t_1 and t_2 as the probabilities that a gamma-ray is captured in the crystal by any means, and the activity A as the total number of disintegrations in the sample, the following equations can be derived (5):

$$A_1 = Ae_1(1-t_2), \tag{7}$$

$$A_2 = Ae_2(1-t_1), \tag{8}$$

$$A_{12} = Ae_1e_2, \tag{9}$$

and

$$T = A(t_1 + t_2 - t_1t_2). \tag{10}$$

Combining the four equations above yields:

$$A = A_1A_2/A_{12} + T. \tag{11}$$

Thus with a single measurement of the gamma spectrum the abso-

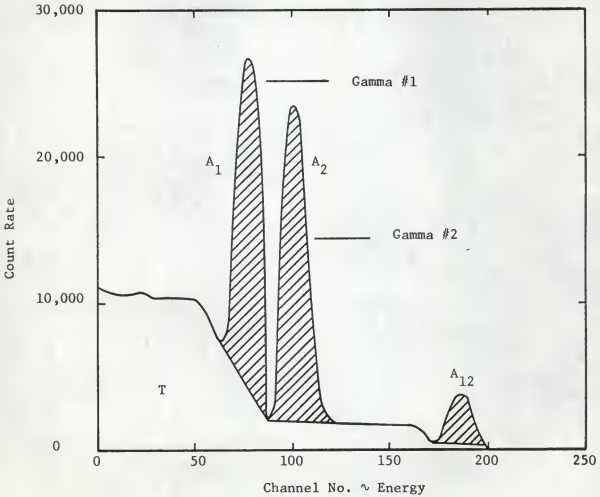

Figure 3. Gamma spectrum of Sc^{46}

lute activity can be determined.

Scandium was chosen as the activation detector for the "sum" peak" technique because it exhibits only two cascading gammas. Methods for treating more complex decay schemes by the "sum peak" method are being developed, but to simplify the calculations it was convenient to use scandium with its simple decay scheme.

Estimates of the errors involved in the three activity determinations by the "sum peak" method indicate an uncertainty of approximately ± 13% for each determination. Two difficulties in the method result in this relatively high error. The first is the uncertainty in calculating areas A_1, A_2, and A_{12} so that they correspond to the quantities represented by equations (7), (8), and (9). Area A_1 is particularly difficult because the Compton contribution from gamma #2 is superimposed on the spectrum in this energy region. The second difficulty results because in practice the first few channels of the analyzer cannot be used. This means that to integrate the entire spectrum, an extrapolation to zero energy in required. This extrapolation may introduce appreciable inaccuracies in T.

Scandium in the form of powdered Sc_2O_3 was irradiated for 30 minutes at the calibration point in the thermal column, and the gamma energy spectrum was obtained using the TMC 4096 Multiparameter system. Numerical integrations were performed to determine areas A_1, A_2, A_{12}, and T from this scandium spectrum. Data obtained from these integrations are given in Table II. Flux values have been corrected for flux depression of the scandium

sample in graphite. The activation cross section for scandium used in the flux calculation is 24 ± 0.1 barns (19), and the average value of neutron flux obtained by the "sum peak" method was (10.47 ± 1.36) x 10^4 n/cm^2-sec-watt.

Table II

Absolute Flux Measurement by the "Sum Peak" Method

Sample No.	A_1 (c/15 min.)	A_2 (c/15 min.)	A_{12} (c/15 min.)	T (c/15 min.)	Initial Activity (A_o dps)	Absolute Flux (n/cm^2-sec-watt x 10^4)
1	265,511	182,246	25,712	1,223,321	3,768	10.98
2	240,834	180,597	25,888	1,216,289	2,515	10.20
3	235,592	276,033	24,649	1,207,652	2,524	10.24

(1.2) Measurement of Thermal, Resonance, and Fast Fluxes in the Central Thimble and the Rotary Specimen Rack

Since the central thimble and the rotary specimen rack are commonly used for a variety of experiments on the TRIGA, it is desirable to provide for the TRIGA user, detailed information about the neutron flux in these facilities. In a thermal reactor neutrons are continuously born in the fission process with energies from 0.05 to 15 Mev. The fission neutrons are slowed down in the moderator material until they reach a state of thermal equilibrium with the moderator molecules. Figure 4 shows the approximate shape of the neutron energy spectrum for a thermal reactor and gives the boundaries of the various flux regions.

Gold, indium, and sulfur induced-activation detectors were irradiated in the central thimble and the rotary specimen rack using the standard polyethylene sample holders provided for this purpose (29). The detectors were positioned 1/8 inch from the bottom of these holders and two 1/8 inch aluminum disks designed to hold the detectors in place. For irradiations in the central thimble the holders were filled with water to prevent perturbations in the flux due to an air gap not ordinarily present in the core at this position. Detectors irradiated in the central thimble were positioned 14 inches below the upper edge of the top grid plate. This position represents the point of maximum flux in the core and is the normal position for irradiations performed in the central thimble. For irradiations in the rotary specimen rack the sample holders were simply lowered into the position directly below the insertion tube.

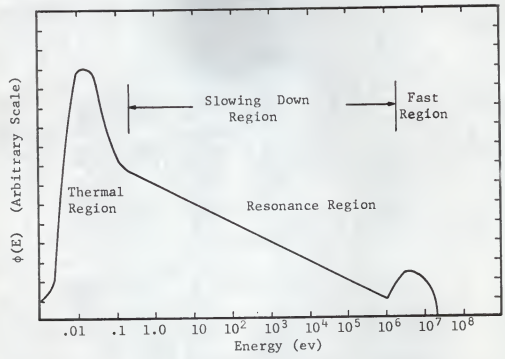

Figure 4. Representative neutron energy spectrum for a thermal reactor.

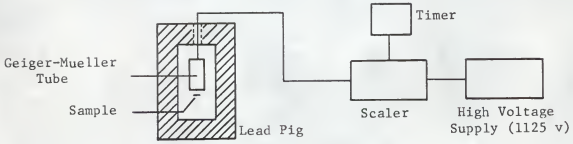

Figure 5. Block diagram of the Geiger-Mueller counting system.

Accurate removal and insertion times were obtained using a Standard Electric Timer (Type SM-60, NE-88). Upon insertion the time was noted, and after the desired amount of irradiation time the sample was pulled from the flux region. The maximum estimated error in this procedure is ± 1.0 seconds for both removal and insertion; therefore, the maximum error in irradiation time is approximately 2.0 seconds.

After removal from the reactor the samples were counted with the Geiger-Mueller counting system represented by the block diagram in Fig. 5. Counting data obtained with this system were used to calculate the initial saturated count rate for each detector. This is accomplished by using the weighted least squares extrapolation program described in Appendix A-1. The Geiger-Mueller system is calibrated for measurement of absolute flux by counting gold foils irradiated in the standard flux in the thermal column.

(2.2-a) Thermal Flux

Gold and indium were chosen as activation detectors for measurement of thermal flux because their activation cross sections are well known, and because 1/v energy dependence can be assumed for both materials in the thermal region. Both gold and indium exhibit large resonance absorption peaks in the slowing down region; thus to separate thermal activity from resonance activity, bare and cadmium covered foils were irradiated in each position. Cadmium 20 mils thick has a high capture cross section for thermal neutrons; however, the cross section drops abruptly

for neutrons with energies greater than 0.5 ev. Consequently the bare foil measures both thermal response and resonance response; whereas, the cadmium covered foil measures only resonance neutrons.

At this point two correction factors need to be considered. One, F_{cd}, accounts for the epithermal absorption of neutrons in cadmium; the other, F_{th}, corrects for flux depression in the vincinity of the foils. Procedure for determining these correction factors is treated in detail in the Handbuch der Physik (2). Values for these corrections applied to detectors used in this work are summarized in Table III.

Table III

Correction Factors For Activation Detectors

Detector	Thickness (mil)	Radius (inches)	Surrounding Medium	F_{cd}	F_{th}
Gold	1	1/2	Water	1.00	1.0168
Gold	1	1/2	Graphite	1.00	1.0032
Gold	5	1/2	Air	1.00	1.0000
Gold	5	1/2	Graphite	1.00	1.0150
Indium	2	1/2	Water	1.05	1.0342
Indium	2	1/2	Air	1.00	1.0000
Indium	2	1/2	Graphite	1.05	1.0035
Scandium	10	1/2	Graphite		1.0035

Applying the above correction factors and subtracting the activity of the cadmium covered foil from the activity of the bare foil yields the following equation for the activity due to thermal neutron flux (2):

$$A_{th} = F_{th}(A_b - F_{cd}A_{cd}), \qquad (12)$$

where

A_{th} = the activity in the foil due to thermal neutrons,

A_b = the activity of the bare foil, and

A_{cd} = the activity of the cadmium covered foil.

(2.2-b) Resonance Flux

The same gold and indium foils used for measurement of thermal flux were also used for the measurement of the slowing down density at specific energies in the resonance region. The single, large resonance peak exhibited by both detectors accounts for most of the activation in the epithermal region, giving an indication of the neutron flux at the resonance energies. The cadmium difference method (22) was then used to establish the 1/E dependence of the spectrum. The cadmium ratio is expressed as

$$R = 1 + \frac{A_{th}}{A_{cd}} . \qquad (13)$$

For a 1/E energy spectrum the ratio ϕ_r/ϕ_{th} will be approximately constant. Ruzik (22) derives the following expression for this ratio:

$$\phi_r/\phi_{th} = \frac{2.37}{(R-1)(1+\alpha)} , \qquad (14)$$

where α is a constant for each material given by

$$\alpha = \frac{\int \sigma_r dE/E}{\int \sigma_{1/v} dE/E} . \qquad (15)$$

If the spectrum is truly 1/E, the differential flux is then given as

$$\phi(E) = \phi_r/E \ . \qquad (16)$$

(2.2-c) Fast Flux

Sulfur was chosen as the threshold detector for measurement of the integrated fast flux in the high-energy part of the neutron spectrum. The reaction of interest, $S^{32}(n,p)P^{32}$, has a saturation cross section of 300 millibarns and an effective threshold energy of 2.9 Mev. (11). The threshold energy of sulfur is established by representing the sulfur cross section as an idealized step function. This step function is zero for all neutron energies below 2.9 Mev. and 300 millibarns for energies above 2.9 Mev. (See Fig. 6)

The sulfur detectors were pressed into pellets 3/16 inch thick and 3/4 inch in diameter. Approximately three grams of USP grade, powdered sulfur was pressed with no binder and no heating at an indicated pressure of 2000 psi on a hydraulic press. A phosphorous pellet of the same dimensions, 3/16 inch thick and 3/4 inch in diameter, was needed for determining the efficiency of the Geiger-Mueller counting system for the P^{32} betas. Amorphorous powdered red phosphorous was pressed at a temperature of 400°C and a pressure of 2000 psi, using approximately four weight percent polystyrene binder. After pressing, the pellets were sprayed with Krylon to prevent flaking.

For calibration of the Geiger-Mueller system the phosphorous pellet was irradiated in the known thermal flux of the ther-

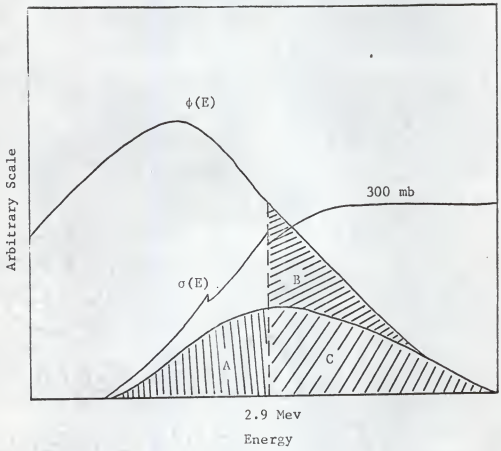

Figure 6. Fission spectrum and cross section for $S^{32}(n,p)P^{32}$ reaction.

Effective threshold energy = 2.9 Mev
Activity of the sulfur detector = Area A + Area C
Integrated fast flux above 2.9 Mev = Area B + Area C
Area A = Area B

mal column and counted with the Geiger-Mueller system. Since the range of the P^{32} betas (E_β = 1.70 Mev.) is considerably less than the thickness of the pellets and since the density of the two materials is nearly the same, it is assumed that the active weight seen by the counting system is the same for phosphorous as for sulfur. With this assumption the following expression can be obtained for fast flux (22):

$$\phi_f = \frac{S_p C_s A_s \sigma_p \phi_{th}}{K_s C_p A_p \sigma_o} \quad . \qquad (17)$$

where

ϕ_f = the integrated fast flux above 2.9 Mev.,

S_p = the content of P^{32} in the phosphorous pellet in weight percent,

K_s = the isotopic content of S^{32},

C_p = the initial saturated count rate from the phosphorous pellet,

C_s = the initial saturated count rate from the sulfur pellet,

A_s = the atomic weight of sulfur,

A_p = the atomic weight of phosphorous,

σ_o = the saturation cross section for the $S^{32}(n,p)P^{32}$ reaction,

σ_p = the activation cross section for P^{31}, and

ϕ_{th} = the thermal flux at the calibration point in the thermal column.

(2.2-d) Tabulated Results for the Central Thimble and the Rotary Specimen Rack

Table IV lists the constants of each detector used in the flux calculations (14, 19, 22). The thermal activation cross

sections are given for a neutron velocity of 2200 meters per second. Alpha is the ratio of the resonance component of the resonance activation to the 1/v component and is defined by equation (15). Table V summarizes irradiation and counting data for foils used in the flux determinations. The detectors irradiated in the thermal column at the flux calibration point were used for the calibration of the Geiger-Mueller system counting system. The results of this calibration for gold foils are given in Table VI. Table VII shows the results of the cadmium difference method for gold and indium detectors. The ratio of ϕ_r/ϕ_{th}, is approximately constant in the central thimble and the rotary specimen rack, indicating that a 1/E spectrum is present.

Table IV

Detector Constants

Detector	Reaction	Activation Cross Section (barn)	α
Gold Au^{197} (2.7 day)	$n + Au^{197} \rightarrow Au^{198}$ β = .960 Mev. (98.6%) γ = .412 Mev. (100%)	98.7	35.4
Indium In^{115} (54.2 min.)	$n + In^{115} \rightarrow In^{116}$	155	37.0
Sulfur S^{32} (14.3 day)	$n + S^{32} \rightarrow P^{32} + p^+$ β = 1.70 Mev. (100%)	Saturated Reaction Cross Section = 0.30	
Phosphorous P^{31} (14.3 day)	$n + P^{31} \rightarrow P^{32}$ β = 1.70 Mev. (100%)	0.23	

Table V

Irradiation and Counting Data

Detector	Position	Indicated Reactor Power Level (watts)	Irradiation Time (minutes)	Weight (grams)	Thickness (mils)	Initial Saturated Counting Rate (cpm/gm)
Au	C. Th.	10	20	.0696	1	$.2024 \times 10^9$
Au*	C. Th.	10	20	.0695	1	$.5830 \times 10^8$
Au	RSR	10	20	.3496	5	$.8027 \times 10^7$
Au*	RSR	10	20	.3514	5	$.1138 \times 10^7$
In	C. Th.	10	3	.0135	2	$.5591 \times 10^9$
In*	C. Th.	10	3	.0185	2	$.1465 \times 10^9$
In	RSR	10	3	.0154	2	$.9237 \times 10^8$
In*	RSR	10	3	.0160	2	$.1626 \times 10^8$
S	C. Th.	10,000	3			$.1047 \times 10^9$
S	C. Th.	1,000	20			$.1012 \times 10^8$
S	RSR	10,000	40			$.3694 \times 10^7$
S	RSR	90,000	5			$.3116 \times 10^8$
Au	Th. Col.	10,000	15	.0695	1	$.4228 \times 10^9$
Au	Th. Col.	10,000	10	.3514	5	$.1107 \times 10^9$
P	Th. Col.	10,000	30			$.1344 \times 10^7$

Table VI

Calibration of the Geiger-Mueller Counting System

Detector	Method of Absolute Flux Determination	Inverse Counter Efficiency (dps/cpm)
Gold (1 mil)	$\beta - \gamma$ Coincidence Method (Au^{198})	37.7
Gold (1 mil)	"Sum Peak" Method (Sc^{46})	43.5
Gold (5 mil)	$\beta - \gamma$ Coincidence Method (Au^{198})	144
Gold (5 mil)	"Sum Peak" Method (Sc^{46})	166

* Indicates cadmium covered foils.

Table VII

Cadmium Difference Method for the
Central Thimble and the Rotary Specimen Rack

Position	Detector	Cadmium Ratio (R)	ϕ_r/ϕ_{th}
C. Th.	Gold (Au^{198})	3.46	.0264
C. Th.	Indium (In^{115})	3.63	.0238
RSR	Gold (Au^{198})	7.06	.0107
RSR	Indium (In^{115})	5.42	.0141

Table VIII

Neutron Flux in the Central Thimble
and the Rotary Specimen Rack

Position	Detector	ϕ_{th} (n/cm^2-sec-watt x 10^7)	ϕ_r (n/cm^2-sec-watt x 10^3)	ϕ_f (n/cm^2-sec-watt x 10^6)
C. Th.	Au	3.14 ± 0.11	20.8 ± 0.7	
C. Th.	S			5.58 ± 0.19
C. Th.	Fission Chamber	3.72* ± 0.18		
C. Th.	Reported** by G.A.	4.0 (<0.21 ev)		6.9 (>2.23 Mev)
RSR	Au	0.562 ± 0.020	0.405 ± 0.015	
RSR	S			0.196 ± 0.007
RSR	Fission Chamber	0.61* ± 0.03		
RSR	Reported** by G.A.	0.72 (<0.21 ev)		0.31 (>2.23 Mev)

* A correction for epithermal fission of the U-235 in the fission chamber should be applied to these flux values before they can be compared to the thermal flux values.

** These values are not reported as Westcott fluxes; therefore, for direct comparison they must be multiplied by the factor $(v_o/\bar{v})$. Also note that the energy ranges of the flux regions are not the same as the energy ranges used for this work.

(1.3) Neutron Flux Mapping in the Reactor Core

The spatial neutron distribution in the TRIGA core was obtained by using a miniature fission chamber as a neutron detector. Access to the core is available through the 0.314 inch foil insertion holes (29) provided in the top grid plate. (See Fig. 7) A fission chamber capable of fitting into these foil insertion holes and of measuring flux in the range from 1×10^8 to 2×10^{14} n/cm^2-second is available commercially from Reuter-Stokes Electronics Components, Inc. of Cleveland, Ohio. The Reuter-Stokes chamber has a sensitive length of 1.0 inch and an outside diameter of 0.250 ± 0.005 inches. The inner electrodes are titanium and the outer shell is 304 stainless steel. The neutron-sensitive portion contains a total of 3.34 milligrams of uranium, 93% enriched in U-235, surrounding an ion chamber filled with helium gas at a pressure of 76 cm. Hg.

Twenty feet of coaxial cable connects the chamber with the associated equipment located on top of the reactor shield. A seal between the active volume of the chamber and the cable prevents gas migration between the detector and the cable, providing uniform sensitivity over temperatures ranging as high as 200°C.

Figure 8 shows the physical arrangement for positioning the fission chamber in the core. A 26 11/16 inch rigid, thin-walled aluminum probe containing the fission chamber slides through the foil insertion holes in the top grid plate. The small hole in the bottom of the probe allows the entire assembly to fill with water. A flexible 20 foot long aluminum guide tube

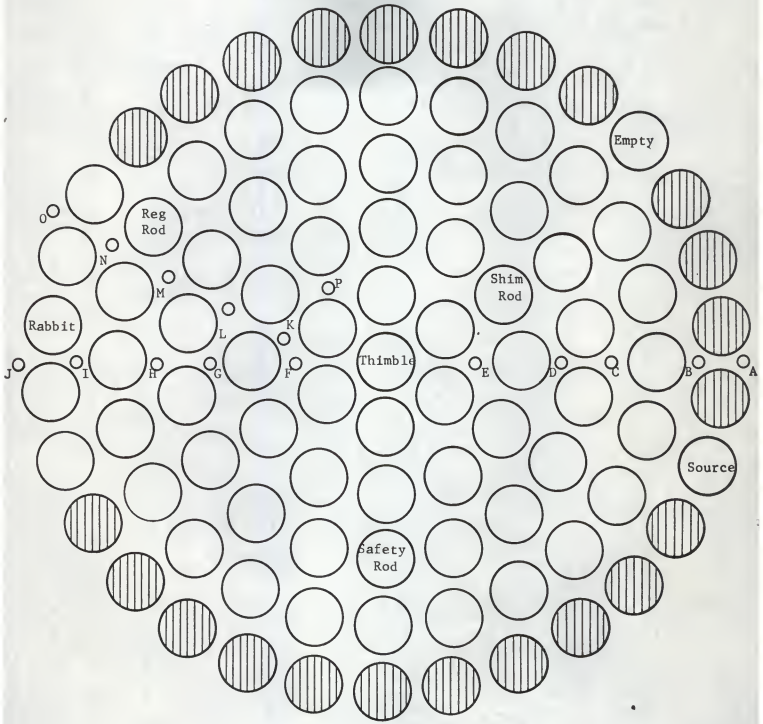

Figure 7. Core loading diagram showing the foil insertion holes.

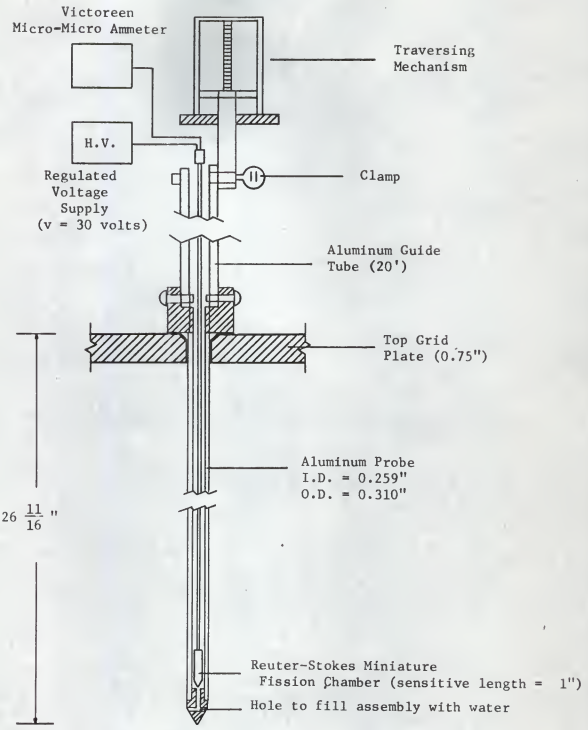

Figure 8. Positioning of the fission chamber in the core

connects the probe to the traversing mechanism on the top of the reactor shield. The flexibility of the guide tube allows access to all the foil insertion holes except I and J despite various obstructions in the pool. Holes I and J are blocked by the terminus assembly of the pneumatic transfer system.

For each vertical traverse the probe containing the fission chamber was completely inserted as shown in Fig. 8. Since the position of the chamber within the probe is fixed and the length of the probe is known, the position of the chamber with respect to the upper surface of the top grid plate is established. With the bottommost position as zero, the probe was pulled upward through the core at the rate of one inch per minute using the traversing mechanism. Current readings were taken with a Victoreen micro-micro ampmeter at 0.50 inch intervals. During each traverse a BF_3 ion chamber positioned two inches above the top grid plate in the central thimble provided an additional check on the stability and reproducibility of the reactor power level.

(1.3-a) Calibration of the Fission Chamber for Measurement of Absolute Neutron Flux

To calibrate the fission chamber for the measurement of absolute flux the chamber response is determined in the region of known thermal flux in the thermal column. Table IX gives the results of this calibration.

Table IX

Current to Flux Conversion Ratio

Method of Absolute Flux Determination	Thermal Flux in the Thermal Column (n/cm^2-sec-watt)	Current Reading of the Fission Chamber (amp/watt)	Factor for Converting* from Current to Flux (nv_o/amp)
$\beta - \gamma$ Coincidence Method (Au^{198})	8.80×10^4	1.30×10^{-12}	0.677×10^{17}
"Sum Peak" Method (Sc^{46})	10.4×10^4	1.30×10^{-12}	0.800×10^{17}
Sensitivity Quoted by Reuter-Stokes			0.67×10^{17}

* This factor has been adjusted to account for the difference between flux depression in graphite and the flux depression in water, using the correction for flux depression as discussed in the Handbuch der Physik (2).

(1.3-b) Discussion of the Neutron Flux Plots in the Core

Figures 9 through 23 are vertical plots of the flux in the central thimble and the 14 flux insertion holes (A through P, excluding I and J). Data for the plots were taken at a reactor power level of 100 watts. This power level is indicated by a reading of $0.33 \times 3 \times 10^2$ watts on the linear recorder on the reactor console. All flux values measured with the fission chamber were corrected for flux perturbations caused by insertion of the chamber into the core.

Figures 24 and 25 show the response of the miniature fission chamber as the reactor power level, indicated by the linear recorder, is varied from 10 watts to 90 kilowatts. The linear recorder (29) has a linear scale from 0 to 11 and a range selector which determines the value of the full scale reading (full scale here refers to a reading of 10 on the linear scale). Figure 24 shows the fission chamber response as the power indicated by the linear recorder is increased over the full scale (0 to 10) at a single range setting. Note that the response is linear with a slope of 0.95 and an intercept of about 0.03 of the full scale reading. The data shown in Fig. 24 were taken at a range selector position of 10×10^1 watts but a similar response was noted for each of the other range selector positions. Thus the power indicated by the fission chamber for any linear recorder position can be read directly from Fig. 24. For example if the linear recorder reads 300 watts (i.e. 0.30 of full scale with a range selector position of 10×10^2 watts), the power indicated by the fission chamber from Fig. 24 is 0.315 of 10×10^2 watts or 315

watts. Figure 25 shows the fission chamber response over the entire power range (10 watts to 90 kilowatts). The data at 10 watts, 100 watts, 1 kilowatt, and 10 kilowatts were taken at 0.33 of full scale with the range selector in the appropriate position. The data at 40 and 90 kilowatts were taken at 0.40 and 0.90 of full scale respectively. For the data at 0.33 of full scale, the slope of the response curve is 1.0. The fission chamber response at 40 and 90 kilowatts, however, indicates a power reading that falls below the extrapolated line of slope 1.0. The slope of the response curve decreases at 40 and 90 kilowatts because the slope of the fission chamber response versus linear recorder power is less than 1.0 as the position of the recorder pen on the linear scale is increased (See Fig. 24).

Throughout this work, fission chamber flux measurements were made at a recorder pen setting of 0.33 of full scale. The only exceptions to this procedure were measurements taken at a linear recorder power level of 90 kilowatts (See Fig. 28 and 29), in which case the pen recorded 0.90 of full scale.

At low power levels (i.e. $\leq$ 10 watts) the gamma radiation resulting from the build up of decaying fission products may contribute significantly to the response of the fission chamber. The magnitude of this effect depends on the operating history of the reactor, but in general for power levels of 100 watts or greater it is small compared to the detector response to neutrons. The above effect is not shown in Fig. 25, but for similar data taken after long, high power operation of the reactor, the fission chamber indicated a significantly higher reading at a linear

recorder power of 10 watts.

The shapes of flux plots are not changed as the power level is increased, except for holes M and N. The shape change in these two holes is a result of the change in the regulating rod position as the power level is increased above 10 kilowatts. Figures 26 and 27 are representative plots of the flux to power ratio for traverses at 100 watts and at 90 kilowatts in hole M and in the central thimble. A result similar to the plot in M can be obtained for hole N, and results similar to the plot in the central thimble can be obtained for the other foil insertion holes. Figures 28 and 29 further indicate the relation of the flux shape to the power level by plotting the fractional difference between the flux to power ratio at 100 watts and 90 kilowatts versus vertical position.

The flux shapes are consistent with what might be expected for the TRIGA core. The entire distribution seems to be shifted slightly downward as a result of the partially inserted neutron absorbing control rods in the upper portion of the core. Sharp flux depressions are noticed locally around the control rods and definite peaking is noticed in the water columns below the control rods and in the central thimble. Flux peaking is also apparent in the graphite end reflectors. The samarium oxide, burnable poison discs located between the fuel and the end reflectors, tend to depress the flux in this region, causing even more pronounced flux peaking in the end reflectors. It should be noted that the flux peaks in the plots obtained with the fission chamber may be appreciably larger and sharper if corrections for the finite resolution of the chamber are considered.

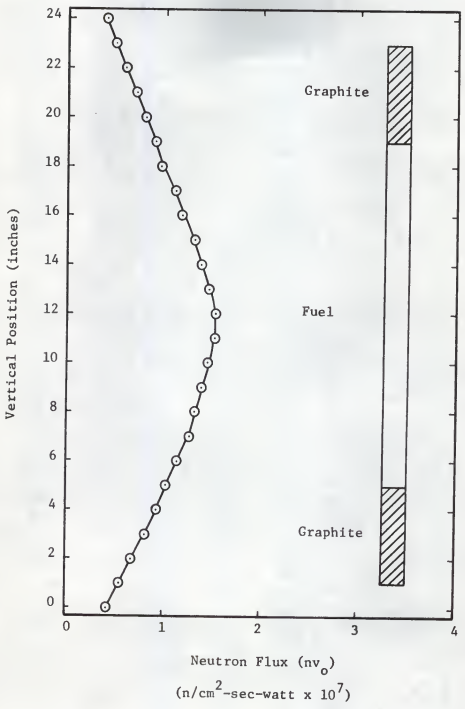

Figure 9. Vertical flux plot in foil insertion hole A

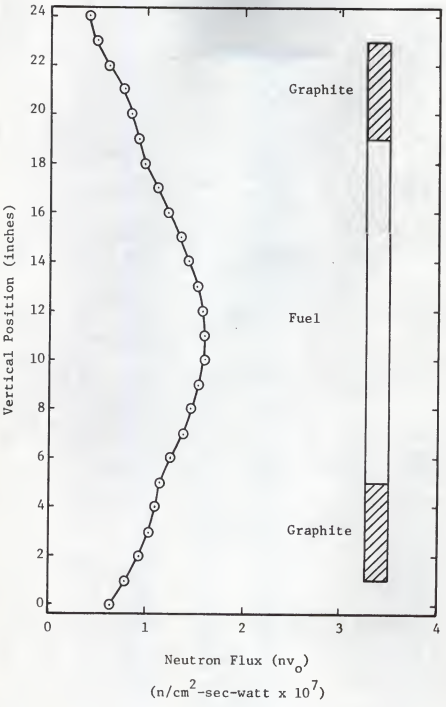

Figure 10. Vertical flux plot in foil insertion hole B

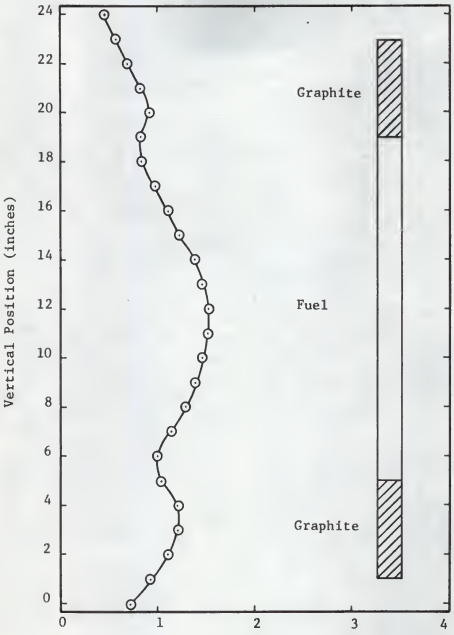

Figure 11. Vertical flux plot in foil insertion hole C

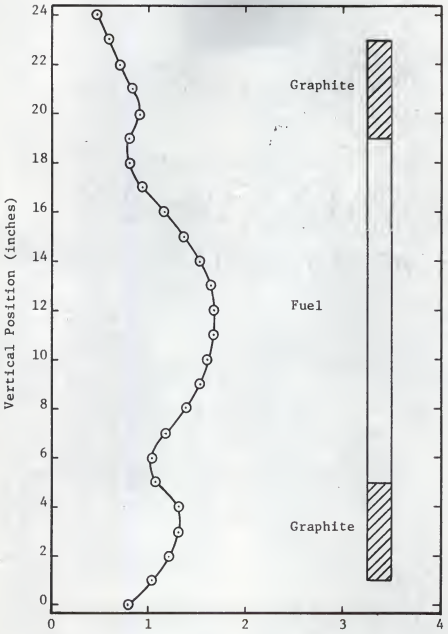

Figure 12. Vertical flux plot in foil insertion hole D

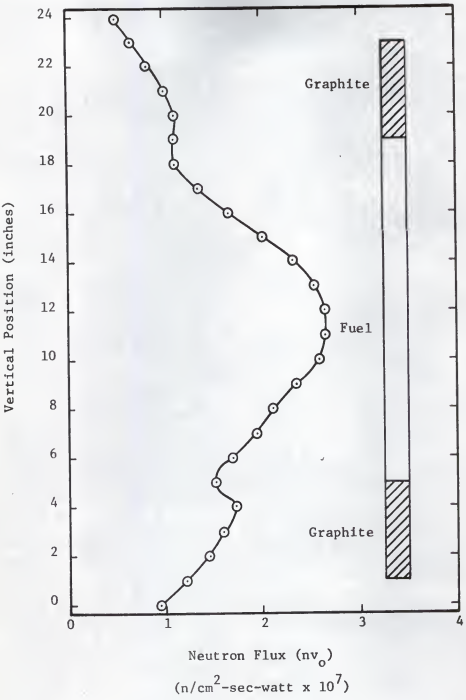

Figure 13: Vertical flux plot in foil insertion hole E

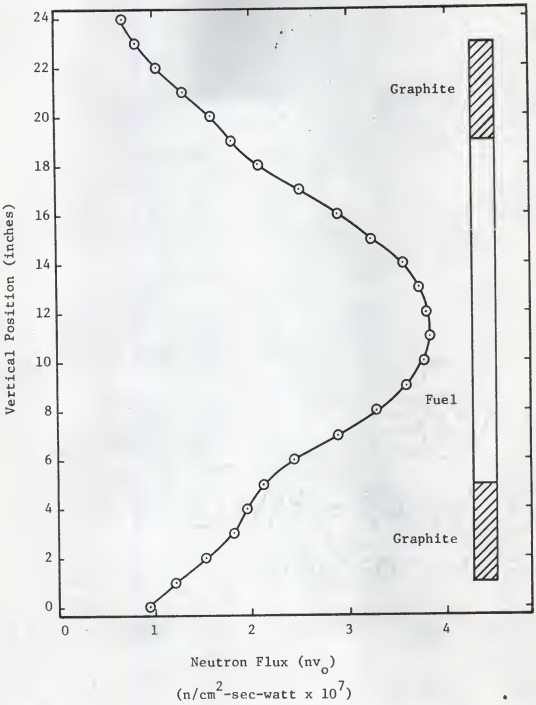

Figure 14. Vertical flux plot in the central thimble.

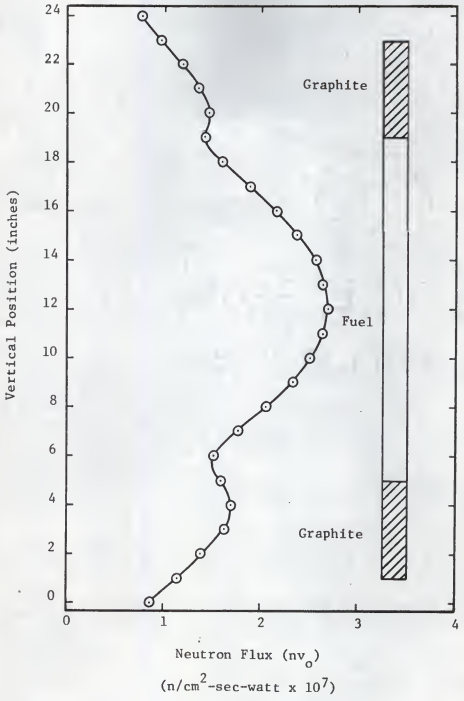

Figure 15. Vertical flux plot in foil insertion hole F

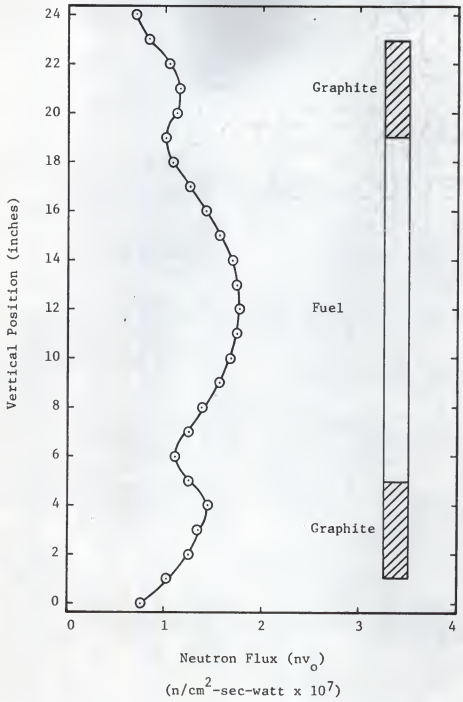

Figure 16. Vertical flux plot in foil insertion hole G

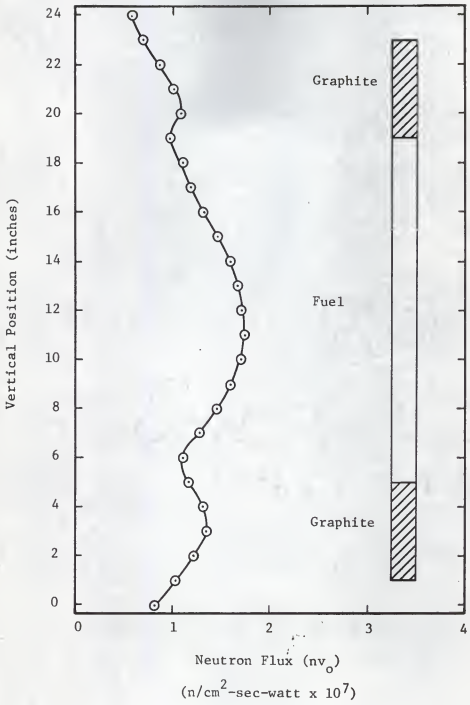

Figure 17. Vertical flux plot in foil insertion hole H

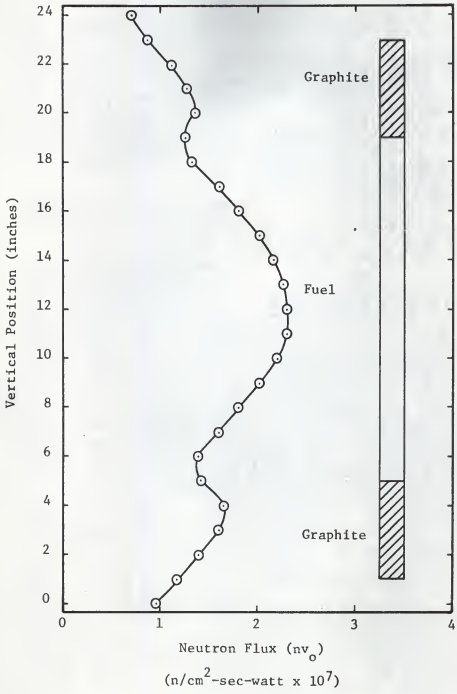

Figure 18. Vertical flux plot in foil insertion hole K

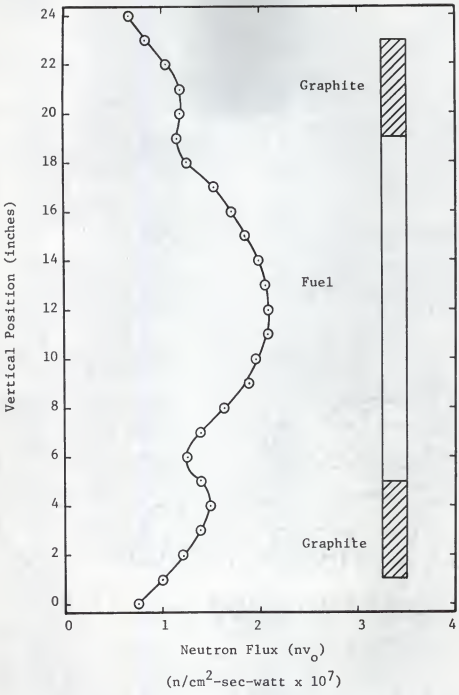

Figure 19. Vertical flux plot in foil insertion hole L

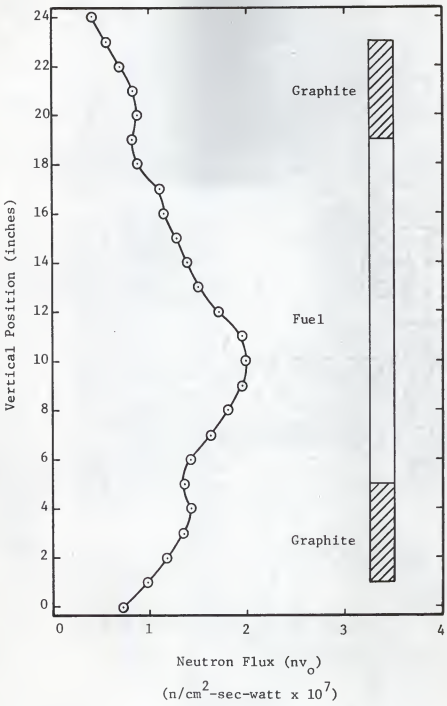

Figure 20. Vertical flux plot in foil insertion hole M

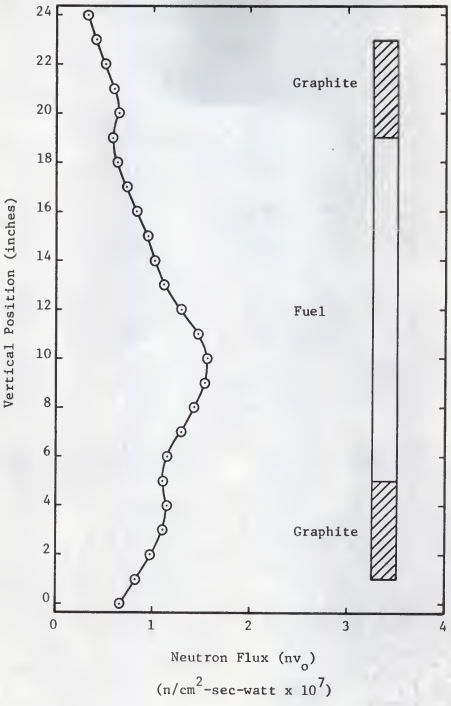

Figure 21. Vertical flux plots in foil insertion hole N

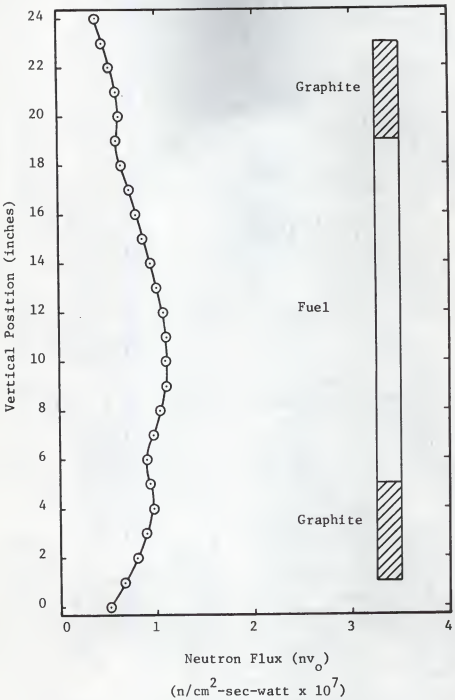

Figure 22. Vertical flux plot in foil insertion hole O

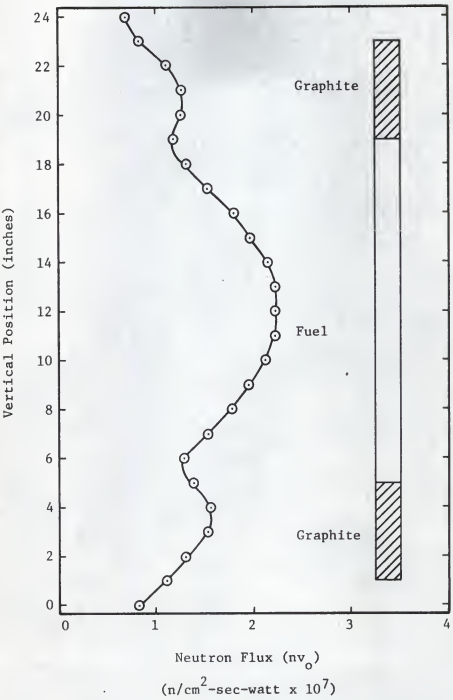

Figure 23. Vertical flux plot in foil insertion hole P

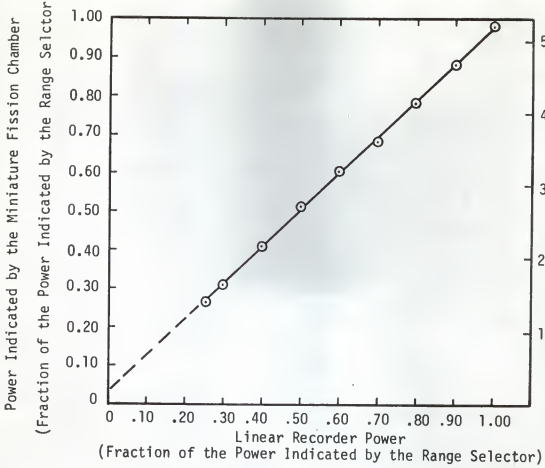

Figure 24. Fission chamber response for a single range on the linear recorder.

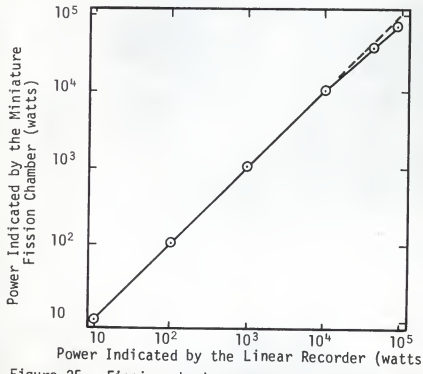

Figure 25. Fission chamber response versus linear recorder power for the power range from 10 watts to 90 kilowatts.

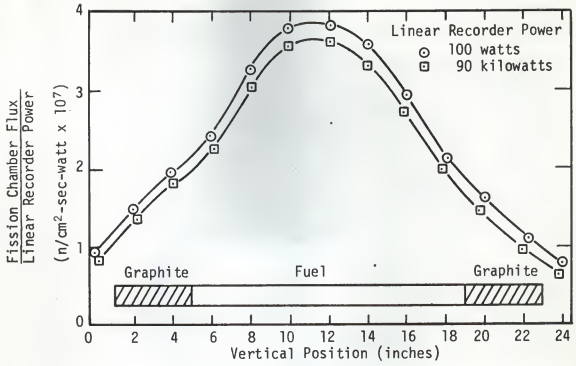

Figure 26. Flux to power ratio in the central thimble.

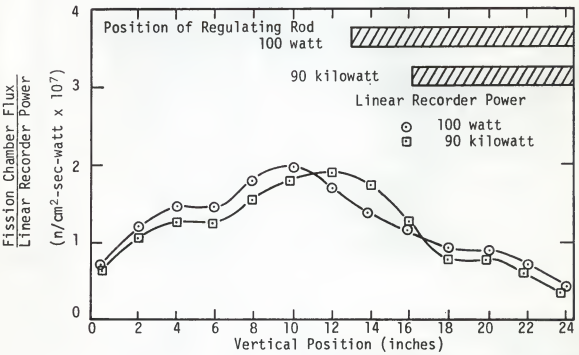

Figure 27. Flux to power ratio in foil insertion hole M near the regulating rod.

$$F = \frac{(\phi/P)_{100 \text{ watts}} - (\phi/P)_{90 \text{ kilowatts}}}{(\phi/P)_{100 \text{ watts}}}$$

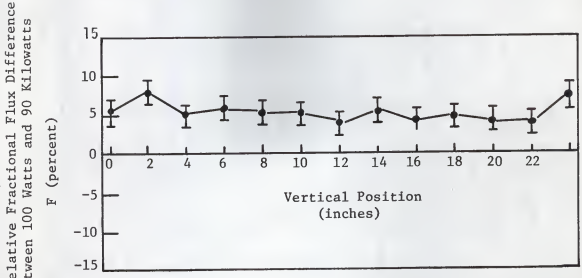

Figure 28. Deviation in flux to power ratio in the central thimble.

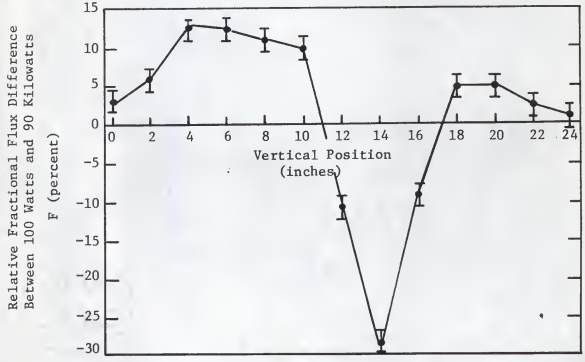

Figure 29. Deviation in flux to power ratio in foil insertion hole M

(2.0) Power Calibration

Measurement of the quantity of heat produced per unit time in the core is essential to the safe control and operation of the reactor. Several power calibrations have been performed on the Kansas State TRIGA using calorimetric methods (i.e., measurement of the increase in water temperature in the reactor pool). These calorimetric methods are adequate; however, measurement of the neutron flux distribution in the core provides an additional means for calculating reactor power level.

Each fission of a U-235 atom releases energy equivalent to 197 ± 8 Mev. or (3.16 ± 0.13) x 10^{-11} watt-sec with the energy distribution given in Table X (21).

Table X

Fission Energy Distribution

Kinetic energy of fission fragments	165	± 5 Mev
Prompt γ-rays	5	
Kinetic energy of fission neutrons	5	± 3
Fission product decay		
Gamma	6	
Beta	5	
Neutrino	11	
Total	197	± 8

This does not, however, represent the total heat energy released in the reactor core region. Some of the fission energy is not converted to heat in the core; instead it escapes the core region in the form of radiation. Further, some additional heat results from capture gammas formed in the core. These effects depend on the reactor geometry and design and are extremely difficult to

calculate. Therefore, in this work the total power generated in the reactor is taken as the total nuclear energy released in the fission process, specifically

$$P = KV\Sigma_f\bar{\phi} \tag{18}$$

where

P = the total power output of the reactor in watts,

V = the volume of U-235 in the core,

Σ_f = the macroscopic fission cross section for U-235 at 2200 meter/second,

$\bar{\phi}$ = the average flux in the fuel region of the core, and

K = the total nuclear energy released per fission in watt-sec/fission.

This value of total nuclear power cannot be compared directly to the calorimetric power generated; however, by simply adjusting the value of K an estimate of calorimetric power output can be obtained. The value of K used to estimate the calorimetric power was $(2.88 \pm 0.20) \times 10^{-11}$ watt-sec per fission.

By assuming that the fission cross section is known for a given quantity of U-235, the problem is reduced to calculating the average flux in the fuel region of the reactor core. The expression for the average flux is

$$\bar{\phi} = \frac{1}{V_c}\int_{V_c} \phi dV \tag{19}$$

where

V_c = the total volume of the fuel in the reactor core, and

ϕ = the neutron flux as a function of position in the reactor.

The above integration is performed numerically by dividing the core into small volume elements as shown in Fig. 30. Each annular volume element is one inch thick and includes one fuel element. The expression for $\bar{\phi}$ then becomes

$$\bar{\phi} = \frac{1}{MN} \sum_{i=1}^{M} \sum_{j=1}^{N} \phi_{ij} \qquad (20)$$

where

ϕ_{ij} = the average flux in the ij^{th} element,

M = the number of vertical levels, and

N = the number of fuel elements.

(3.1) Ratio of the Maximum Flux in the Moderator to the Average Flux in the Fuel

In a heterogeneous reactor such as the TRIGA Mark II it is not practical to measure directly the neutron flux within the fuel element. Instead the flux measurements were made with the miniature fission chamber in the water region between the fuel elements. From these measurements the average flux in a fuel element for a particular horizontal level is obtained by averaging the flux values at the four corners of an annular element and by multiplying this average by the ratio of the maximum flux in the water moderator to the average flux in the fuel. This ratio is approximately equal to the disadvantage factor ζ and can be estimated as the absorption cross section of the hydrogen in the water divided by the absorption cross section of the hydrogen in

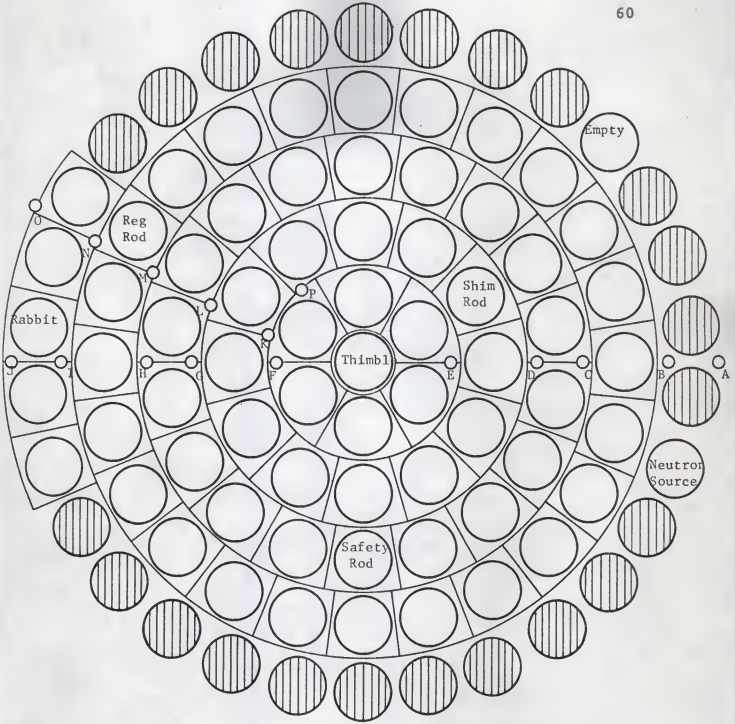

Figure 30. Loading diagram showing the annular elements. (Note that the core was divided similarly for each of the 14 different vertical levels.)

the fuel. By using the cross section for the TRIGA given by West (31) the value of the disadvantage factor is approximately 1.37.

(3.2) Flux Perturbations Near the Control Rods and the Central Thimble

For proper calculation of the average flux in the core some correction must be made for changes in the neutron flux distribution resulting from various irregularities in the core lattice. During normal operation of the Kansas State TRIGA, one control rod, the pulse-safety rod, is completely withdrawn from the core, but the regulating and the shim rods are partially inserted. By assuming that there is a flat neutron distribution in the area of these control rods and that there is absorption of only thermal neutrons, flux depressions near the surface of the rods and flux peaking near the water columns below the control rods and in the central thimble can be calculated from the following expression (14):

$$\phi = \phi_o \left[1 - BK_o(\kappa r)/\phi_o \right] \qquad (21)$$

where

ϕ = the neutron flux in the vicinity of the control rod,

ϕ_o = the neutron flux in an unperturbed region,

B = the experimentally determined proportionality constant for the effects of a control rod on neutron flux,

$\kappa = 1/L_{th}$,

L_{th} = the thermal diffusion length in the core,

r = the distance from the center of the control rod, and

$K_o(\kappa r)$ = the modified Bessel function of the second kind of zero order.

Experimental data obtained with the miniature fission chamber can now be used to calculate values for B at various vertical levels near a control rod. Solving equation (21) for B yields

$$B = \frac{\phi - \phi_o}{K_o(\kappa r)} . \qquad (22)$$

By using flux values from flux insertion hole M for ϕ and flux values from hole H for ϕ_o, experimental B values are obtained for the regulating rod. Although similar measurements of B cannot be done for the shim and the pulse-safety rod, it is possible to get a good approximation for B for these rods, assuming (1) proportionality between B and the rod worth and (2) water columns in all three rods have the same negative B values.

(2.3) Reactor Power Level

An IBM computer code described in Appendix (A-2) is used for calculation of the average neutron flux in the fuel. This program uses flux data obtained with the miniature fission chamber and accounts for both the disadvantage factor correction and the correction for flux perturbations near the control rods and the central thimble. The results of the average flux calcula-

tions and the values for reactor power level calculated from equation (18) are summarized in Table XI. Detailed numerical calculations of the reactor power level and an estimate of the uncertainty associated with these calculations are performed in Appendix (A-2).

Table XI

Power Calibration

Method of Absolute Flux Calibration	Average Flux in the Fuel $\bar{\phi}$ (n/cm^2-sec-watt x 10^7)	Total Nuclear Power (watts)	Estimated Calorimetric Power (watts)	Estimated Uncertainty (%)
$\beta - \gamma$ Coincidence Method (Au^{198})	1.03 ± 0.08	1.12 ± 0.10	1.03 ± 0.11	10.4
"Sum Peak" Method (Sc^{46})	1.22 ± 0.18	1.34 ± 0.20	1.22 ± 0.20	16.1

(3.0) Summary of Results

Figures 31 and 32 are two dimensional contour plots summarizing neutron flux data taken with the fission chamber. Figure 31 shows the flux contour in a relatively unperturbed region, and Fig. 32 shows the contour on a plane passing near the regulating rod. Table XII applies to both Fig. 31 and 32. The contour lines were drawn by hand with no attempt to interpolate between data points.

These plots are presented in this manner so that they can be compared to similar plots presented by West (31). Figure 33 is a two dimensional plot reproduced from West's report and applies to a TRIGA Mark I or II core containing 56 fuel elements and four completely withdrawn control rods. Table XIII applies to this figure. This plot should not be compared directly to the experimental data for a number of reasons. First, the neutron flux in Fig. 33 is defined by $\phi = n\bar{v}$ rather than by "Westcott convention," $\phi = nv_o$. Second, flux in Fig. 33 is given for the homogenized core as calculated by West; whereas, the experimental data are taken with the fission chanber in the water gaps between the elements. Third, the plot from West is for thermal flux (i.e., 0 to 0.05 ev), but the experimental data have not corrected for epithermal fission of U-235 in the chamber and does not, therefore, represent strictly thermal flux.

Experimental flux values measured in various positions in the Kansas State TRIGA are summarized in Table XIV. The values

reported in this Table are calculated by using the beta-gamma coincidence method for calibration of absolute flux.

Table XII

Neutron Flux for the Experimental Two Dimensional Contour Plots (Figures 31 and 32)

Contour Line No.	Westcott Flux Measured with the Fission Chamber (n/cm^2-sec-watt x 10^7)
4	0.500
5	0.625
6	0.750
7	0.875
8	1.000
9	1.125
10	1.250
11	1.375
12	1.500
13	1.625
14	1.750
15	1.875
16	2.000
17	2.125
18	2.250
19	2.375
20	2.500

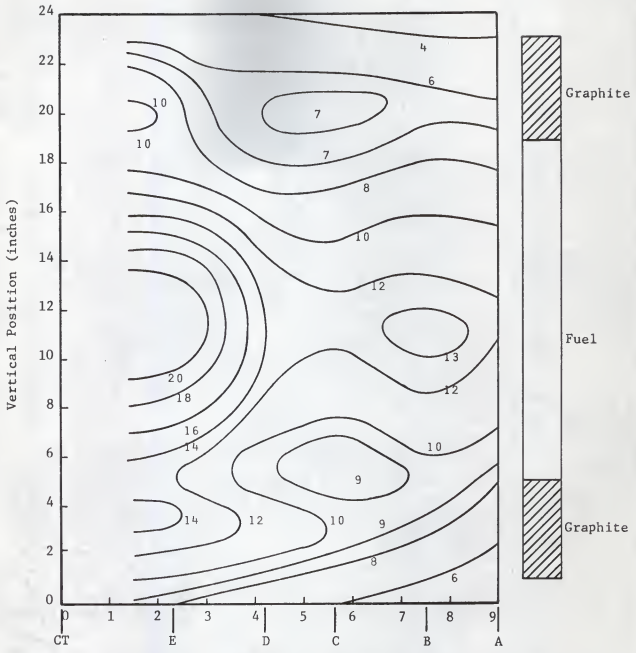

Figure 31. Two dimensional flux contour of the TRIGA core measured with the miniature fission chamber.

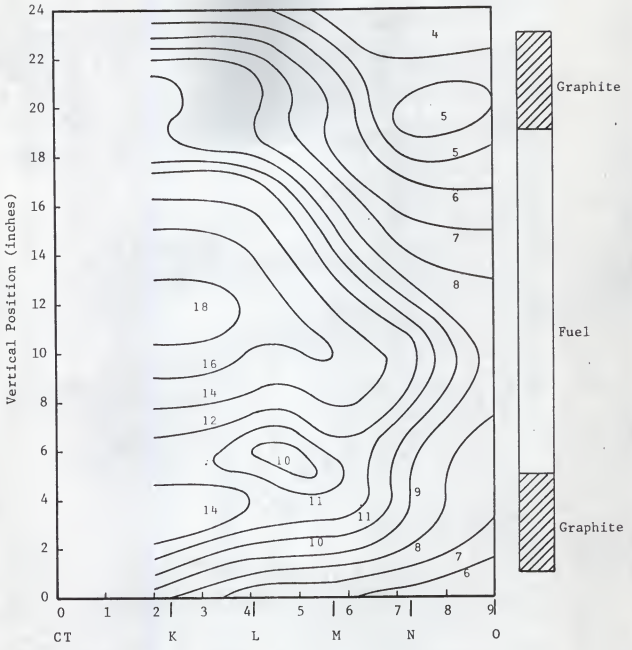

Figure 32. Two dimensional flux contour of the TRIGA core measured with the miniature fission chamber.

Table XIII

Neutron Flux for the Two Dimensional
Contour Plot Reproduced From West (31)
(Figure 33)

Contour Line No.	Thermal Neutron* Flux (n/cm^2-sec-watt x 10^7)
0	0.500
1	0.550
2	0.600
3	0.650
4	0.700
5	0.750
6	0.800
7	0.850
8	0.900
9	0.950
10	1.000
11	1.050
12	1.100

* Neutron flux as used by West is defined as $\phi = n\bar{v}$ rather than by "Westcott convention".

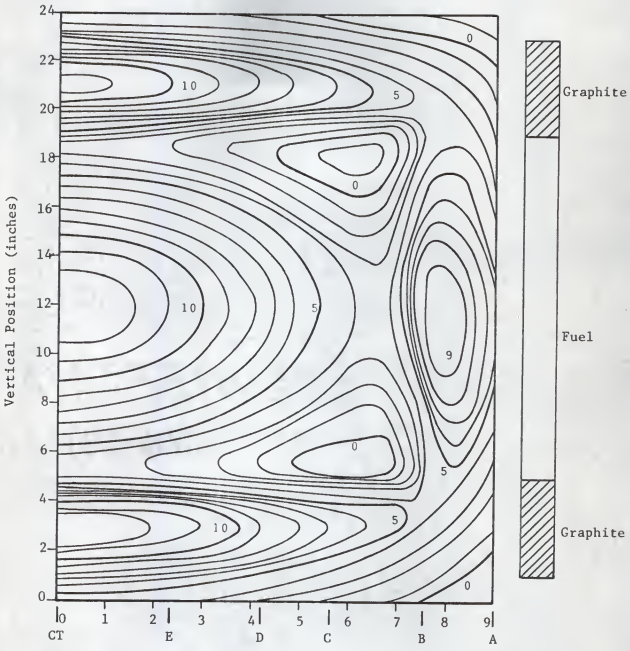

Figure 33. Two dimensional thermal flux contour as presented by West (31).

Table XIV

Neutron Flux in the TRIGA Mark II *
Irradiation Facilities

Position	ϕ_{th}** (< 0.5 ev) (n/cm^2-sec-watt)	ϕ_r** (n/cm^2-sec-watt)	ϕ_f*** (> 2.9 Mev) (n/cm^2-sec-watt)
Central Thimble	$(3.14 \pm 0.11) \times 10^7$	$(2.08 \pm 0.07) \times 10^4$	$(5.58 \pm 0.19) \times 10^6$
Rotary Specimen Rack	$(5.62 \pm 0.20) \times 10^6$	$(4.05 \pm 0.15) \times 10^1$	$(1.96 \pm 0.07) \times 10^5$
Calibration Point in the Thermal Column	$(8.80 \pm 0.25) \times 10^4$		

* "Westcott convention" is used in reporting all flux values.

** Thermal and resonance flux values are obtained using gold activation detectors.

*** Fast flux values are obtained using sulfur threshold detectors.

(4.0) Suggestions for Further Study

It is suggested that additional work be performed to improve the accuracy of the absolute flux measurements at the calibration point in the TRIGA thermal column. Improvement of the beta-gamma coincidence technique is suggested through the use of a high efficiency beta detector and more sophisticated pulse shaping circuitry. Further development of the "sum peak" method is also suggested, with particular emphasis on methods for calculating the areas under the photopeaks.

For this work thermal, resonance, and fast flux measurements were performed only in the central thimble and the rotary specimen rack. Similar measurements could be made for the other irradiation facilities of the TRIGA Mark II (i.e., the pneumatic transfer system and the four beam ports).

The detailed experimental flux plots obtained using the Reuter-Stokes fission chamber may be compared with the neutron flux calculated by various analytical methods. When the IBM-360 computer is installed at Kansas State it should be feasible to perform large multi-group calculations to obtain flux plots similar to those presented by West (31). It might also be feasible to devise a two dimensional code which calculates the flux perturbations near the control rods and the other irregularities in the core. These computer codes could then be used to calculate the flux shapes for the actual core loading in the Kansas State TRIGA for various control rod positions and compared directly to the experimental flux.

(5.0) Acknowledgment

The author wishes to express his gratitude to Dr. M. Copic for his guidance and help throughout the course of this study. Sincere appreciation is given to the Department of Nuclear Engineering for their financial support which made this study possible, and special thanks is given to Mr. R. W. Clack and the operating staff of the Kansas State TRIGA for their cooperation in scheduling and performing these experiments. I also wish to thank Mr. Dean Eckhoff, Mr. Robert Ihde, and Mr. Glen Correll for their suggestions and particular contributions.

LITERATURE CITED

1. Abson, W., P. G. Solmon, and S. Pyrah
"The Design, Performance, and the Use of Fission Counters," The Institute of Electrical Engineers. Paper No. 2546M, (1958).

2. Amaldi, E.
Handbuch der Physik. Vol. 38, Part II, Berlin: Springer, 1959.

3. Barnothy, J. and M. Forro
"Coincidence Methods of Measuring Disentegration Rates of Radioactive Sources," Review of Scientific Instruments. 22, 415, (1951).

4. Baum, J. B.
Neutron Dosimetry - A Review. UR-381, 1955.

5. Brinkman, G. A., A. H. W. Aten, Jr., J. Th. Veenboer, and W. G. Zylstra.
"Absolute Standardization with a NaI(Tl) Crystal by Means of the 'Sum Peak' Method for Calibration of Lu^{176}," Symposium on Radioisotopes Sample Measurement Techniques in Medicine and Biology. Vienna, Austria, (1965).

6. Brinkman, G. A., A. H. W. Aten, Jr., and J. Th. Veenboer
"Absolute Standardization with a NaI(Tl) Crystal--I, Calibration by Means of a Single Nuclide," International Journal of Applied Radiation and Isotopes. 14, 153-157, (1963).

7. Brinkman, G. A., A. H. W. Aten, Jr., and J. Th. Veenboer
"Absolute Standardization with a NaI(Tl) Crystal--II, Determination of the Total Efficiency," International Journal of Applied Radiation and Isotopes. 14, 433-437, (1963).

8. Brinkman, G. A., A. H. W. Aten, Jr., and J. Th. Veenboer
"Absolute Standardization with a NaI(Tl) Crystal--IV Determination of Photoelectric Efficiency," International Journal of Applied Radiation and Isotopes. 16, 15-18, (1965).

9. Campion, P. G.
"The Standardization of Radioisotopes by the Beta-Gamma Coincidence Method Using High Efficiency Detectors," International Journal of Applied Radiation and Isotopes. 4, 232-248, (1959).

Literature Cited (cont.)

10. Campion, P. G., and J. G. V. Taylor
International Journal of Applied Radiation and Isotopes. 10, 131, (1961).

11. Cola, G. D., and A. Rota
"Calculation of Differential Fast Neutron Spectra from Threshold Foil Activation Data by Least-Squares Series Expansion Methods," Nuclear Science and Engineering. 23, 344-353, (1965).

12. DeVolpi, A., K. A. Porges, and R. N. Larsen
Mn^{56} Coincidence Counting Facility. ANL-6760, (1963).

13. Dragoumis P., J. R. Weir, and G. W. Leddicotte
Fast Flux Measurements in the ORR Core. ORNL-3028, (1961).

14. Etherington, H.
Nuclear Engineering Handbook. New York: McGraw-Hill Book Company, Inc., 1958.

15. Galanin, A. D.
Thermal Reactor Theory. New York: Pergamon Press, 1960.

16. Glasstone, S. and M. C. Edlund
The Elements of Nuclear Reactor Theory. New York: D. Van Nostrand Company, Inc., 1952.

17. Hazards Summary Report for the Kansas State University TRIGA Mark II Reactor. Compiled by the Department of Nuclear Engineering, Manhattan, Kansas, (1961).

18. Hughes, D. J.
Neutron Pile Research. Reading, Mass.: Addison-Wesley, 1953.

19. Hughes, D. J. and R. B. Schwartz
Neutron Cross Sections. BNL-325, (1958).

20. Kansas State University TRIGA Mark II Reactor Logbook. (November 22, 1966).

21. Leonard, B. E. and E. J. Story
Nuclear Reactor Power Calibration by the Integrated Flux Method. North Carolina State College, Rayleigh, North Carolina, Physical Sciences Research, Technical Report No. 1, (1961).

Literature Cited (concl.)

22. A Manual of Reactor Laboratory Experiments. ANL-6990, (1965).

23. Price, W. J.
Nuclear Radiation Detection. New York: McGraw Hill Book Company, 1964.

24. Sieghbahn, Kai
Alpha-, Beta-, and Gamma-Ray Spectrometry. Vol. 1, Amsterdam, Holland: North-Holland Publishing Company, 1965.

25. Stentz, R. H. and R. L. Treinen
Final Report - Development of Nuclear Sensors. GEMP-90, (1965).

26. Technical Foundations of TRIGA, GA-471, 1958.

27. Trice, J. B.
Fast Neutron Flux Measurements in E-25 of the Brookhaven Graphite Reactor. ORNL-CF-55-7-130, (1955).

28. Trice, J. B.
"Measuring Reactor Spectra with Thresholds and Resonances," Nucleonics. 16 (7), 81-83, (July, 1958).

29. TRIGA Mark II Reactor Mechanical, Maintenance, and Operating Manual. GA-1444, (1960).

30. Typical Experiments for the TRIGA Mark II. GA-386, (1958).

31. West, G. B.
Calculated Fluxes and Cross Sections for TRIGA Reactors. GA-4361, (1963).

32. Westcott, G. H., W. H. Walker, and T. L. Alexander
"Effective Cross Sections and Cadmium Ratios for the Neutron Spectra of Thermal Reactors," Second United Nations International Conference on the Peaceful Uses of Atomic Energy. 16, 70-75, (1958).

APPENDIX

(A-1) Weighted Least Squares Analysis for Calculating Initial Count Rate

The count rate at time t of a decaying radioisotope is given by the relation

$$\ln C = -\lambda t + \ln C_o \qquad \text{(A-1)}$$

where

C = the count rate at time t,

C_o = the initial count rate,

λ = the radioactive decay constant of the isotope, and

t = the time after the initial count rate.

The program described here fits the linear relation of equation (A-1) to a series of count rates using a weighted least squares method. The error associated with each count rate is given by

$$\delta_i = \frac{1}{\sigma_i^2}[\ln C_i - (-\lambda t_i + \ln C_o)]. \qquad \text{(A-2)}$$

In this method the sum of the errors squared is written as

$$E = \sum_{i=1}^{n} \delta_i^2 = \sum_{i=1}^{n} \frac{1}{\sigma_i^2}(\ln C_i + \lambda t_i - \ln C_o)^2 \qquad \text{(A-3)}$$

where

n = the number of count rates in the fit,

$\frac{1}{\sigma_i^2}$ = a weighting factor for the i^{th} count rate,

σ_i = the variance on the count rate after correction for background and dead time.

Since λ is a known value, it is held constant and the least squares criterion is satisfied by choosing $\ln C_o$ such that E is

a minimum. This minimization is done by taking the derivation of E with respect to $\ln C_o$ and setting this derivation equal to zero as follows:

$$\frac{dE}{d(\ln C_o)} = 0 = 2\sum_{i=1}^{n}\frac{1}{\sigma_i^2}(\ln C_i + \lambda t_i - \ln C_o)(-1) \qquad \text{(A-4)}$$

Solving for the $\ln C_o$ yields

$$\ln C_o = \frac{\sum_{i=1}^{n}\frac{1}{\sigma_i^2}(\lambda t_i + \ln C_i)}{\sum_{i=1}^{n}\frac{1}{\sigma_i^2}}, \qquad \text{(A-5)}$$

and the initial count rate is found by simply taking the antilogrithm of equation (A-5). The variance of the initial count rate C_o is calculated from the expression

$$\sigma_{C_o}^2 = \frac{C_o^2\sum_{i=1}^{n}\frac{1}{\sigma_i^2}(\ln C_o - \lambda t_i - \ln C_i)^2}{[n-1]\sum_{i=1}^{n}\frac{1}{\sigma_i^2}}. \qquad \text{(A-6)}$$

As a check to determine whether or not the isotope is decaying at the expected half life, the program also performs a two parameter fit using the least squares technique and solves for the radioactive decay constant λ. In addition to the least squares analysis, the program corrects for the background counting rate, the dead time of the counting system, and the decay of the isotope during a finite counting time. The dead time calculated for the Geiger-Mueller counting system described in section

(1.2) was 172.8 micro seconds. The final result of the program is the initial saturated count rate in units of counts/minute-gram.

Fortran Program for Calculation of Initial Counting Rates

```
HOWES      JOB, INITIAL ACTIVITIES
HOWES      COST 15 MINUTES, 1 PAGES, HOUGHEY, M. E. DEPT.
HOWES      ASGN TU8,12
HOWES      ASGN MGO,16
MEMBER      CDE GO,TEST
HOWES      EXEC FORTRAN.......EXTRAW
   DIMENSION AC(8),AF(10),TILPLI(10),D(3)
 1 FORMAT(2E20.8)
 2 FORMAT(I1 ,3F10.1,I10)
 4 FORMAT(8A10)
   FORMAT(6F10.1)
11 FORMAT(24HKINDICATED HALF-LIFE IS,E14.8,5H MIN.)
12 FORMAT(29HTINITIAL SPECIFIC COUNT RATE=,E14.8,7H CPM/G,5X,10HDEVI
  2ATION=,E14.8)
13 FORMAT(60HTINITIAL COUNT RATES NORMALIZED TO INFINITE IRRADIATION
  2TIME)
   READ(1,1)TAU,ETAU2
   READ(1,2)NFOIL
   WRITE(3,13)
   DO3M=1,NFOIL
   READ(1,4)AC
   WRITE(3,4)AC
   READ(1,2)NTC,TIR,FMASS,TC,WAT
   SPC=0.
   SPCT=0.
   ST=0.
   ST2=0.
   SWF=0.
   ALOG=1.
   SFMU=0.
   GOTO(5,6,7),WAT
 5 A=ALOG(2.)/(2.78*24.*60.)
   GOTO8
 6 A=ALOG(2.)/54.2
   GOTO8
 7 A=ALOG(2.)/(14.3*24.*60.)
 8 TA=ALOG(A*TC/(1.-EXP(-A*TC)))/A
   READ(1,11) D(1),D(2),D(3)
   DO9K=1,NTC
   READ(1,2)IC,TD,TH,TM,SO,TR
   T=60.*(24.*TD+TH)+TM+TA
   C=C /(TC-CO*TAU)-SO/(TC-CO*TAU)
   COF=1./(TC-CO*TAU)**2
   BUF=1./(TC-SO*TAU)**2
   WF(K)=1./D(K)**2
```

```
      EC=ALOG(C)
      SEC=SEC+EC
      SECT=SECT+EC*T
      ST=ST+T
      SWF=SWF+WF(K)
      TILPLI(K)=A*T+EC
      SFNL=SFNL+WF(K)*TILPLI(K)
      ST2=ST2+T*T
      RNTC=NTC
      RL=SFNL/SWF
      A=EXP(RL)/(FMASS*(1.-EXP(-A*TIR)))
      THALF=-ALOG(2.)*(RNTC*ST2-ST*ST)/(RNTC*SECT-ST*SEC)
      WRITE(3,11)THALF
      DO14K=1,NTC
   14 SESQ=SESQ+WF(K)*(RL-TILPLI(K))**2
      IDEV=A*SQRT(SESQ/(SWF*(RNTC-1.)))
    3 WRITE(3,12)A,IDEV
      STOP
      END
$ MON14       EXEC LINKLOAD
              CALL EXTMAPL
  MON14       EXEC EXTMAPL,MJB
```

(A-2) Calculation of Reactor Power Level by the Integrated Flux Method

To calculate the power generated in the TRIGA core the average flux in the fuel portion of the core, $\bar{\phi}$, is determined from the thermal flux data taken with the miniature fission chamber. To calculate this average flux the core is divided into annular elements as shown previously in Fig. 30. The average flux is then approximated by the expression

$$\bar{\phi} = \sum_{i=1}^{14} \sum_{j=1}^{N} \phi_{ij} \qquad \text{(A-7)}$$

where i indicates the vertical level, ϕ_{ij}, is the average flux in the ij^{th} volume element, and N is the number of fuel elements. The average flux in a volume element, ϕ_{ij}, is obtained by estimating from the geometry of the core and from the measured values, the flux at each of the four corners of the annular element and by taking the average of these values divided by the disadvantage factor. The computer program presented at the end of this appendix corrects the flux data for flux perturbations near the central thimble and the three control rods, and performs the numerical integration described above. Flux data taken at eight different radial positions (foil insertion holes B, C, F, G, H, K, O, and the central thimble) are used in the program. These positions were chosen because they represent positions where control rod effects are relatively small.

The values of B used for the flux perturbation calculations are given in Table XII. The B values for the regulating rod

were determined experimentally by using equation (22) with data from foil insertion hole H as unperturbed flux values and data from foil insertion hole M as perturbed flux values. The B values for the shim and the pulse-safety control rods and for the central thimble were estimated from the B values calculated for the regulating rod.

Table XII

Calculation of the Experimental Constant B in the Equation $\phi = \phi_o(1 - BK_o(\kappa r)/\phi_o)$

Vertical Level	Regulating Rod ($\times 10^7$)	Shim Rod ($\times 10^7$)	Pulse-Safety Rod ($\times 10^7$)	Central Thimble ($\times 10^7$)
1	0.77	2.00	-0.77	-0.77
2	0.95	2.25	-1.35	-1.35
3	0.95	2.45	-1.71	-1.71
4	1.15	-0.55	-1.90	-1.90
5	1.15	-1.75	-1.90	-1.90
6	0.59	-1.70	-1.90	-1.90
7	-0.55	-1.90	-1.90	-1.90
8	-1.53	-1.90	-1.90	-1.90
9	-1.54	-1.90	-1.90	-1.90
10	-1.92	-1.90	-1.90	-1.90
11	-1.90	-1.90	-1.90	-1.90
12	-1.71	-1.71	-1.71	-1.71
13	-1.35	-1.35	-1.35	-1.35
14	-0.77	-0.77	-0.77	-0.77

As shown by equation (18) the power generated in a reactor is simply the fission rate in the core times the volume of fuel in the core times the energy released per fission. However, for the calculation of power it is convenient to rewrite equation (18) as

$$P = \frac{KN_a m\sigma_f}{A_{235}} \bar{\phi} \qquad (A\text{-}8)$$

where

m = the mass of the U-235 in the core,

A_{235} = the atomic weight of U-235,

σ_f = the microscopic fission cross section,

N_a = Avogadro's number, and

K = the energy released per fission.

Substituting the proper numerical values into equation (A-8) yields:

$$P = \frac{(2.88 \times 10^{-11})(0.6023 \times 10^{24})(2325)(580 \times 10^{-24})(1.03 \times 10^{7})}{(235)}$$

$$P = 1.03 \text{ watts.}$$

where the value for $\bar{\phi}$ was obtained using the beta gamma coincidence method for determining absolute flux and has been corrected for the ratio of the maximum flux in the water to the average flux in the fuel. The microscopic fission cross section for U-235 at 2200 meters per second was taken as 580 ± 7 barns. Factors for correcting the cross section for departure from the 1/v form are tabulated by C. H. Westcott in Effective Neutron Cross Sections. Since this publication was not available the 2200 meters per second cross section was assumed. It is estimated that this correction would lower the effective cross section by somewhat less than 2%. It is not necessary to correct the cross section for the epithermal component of the neutron spectrum because the flux data was not corrected for epithermal fission in the fission chamber.

To obtain an estimate of the inaccuracies in the power calibration each of the quantities in equation (A-8) are consid-

ered separately. The values for Avogadro's number, the mass of the fuel present in the core, and the atomic weight have negligible uncertainty compared to the other quantities. The total nuclear energy released per fission is $(3.16 \pm 0.13) \times 10^{-11}$ watt-sec./fission. Additional uncertainty results in this constant when estimating the actual calorimetric power output. The value of K in this case becomes $(2.88 \pm 0.20) \times 10^{-11}$ watt-sec./fission. The microscopic fission cross section as already stated is 580 ± 7 barns. The final uncertainty in the power calculation results from the difficulty in calculating the average flux in the fuel. An estimate of the statistical deviation on the average flux in the fuel can be obtained from the following expression:

$$\sigma^2_{\bar{\phi}} = \frac{1}{V^2} \sum_{i=1}^{14} \sum_{k=1}^{M} V_k^2 \sigma^2_{\phi_{ik}} . \qquad \text{(A-9)}$$

where

$\sigma^2_{\bar{\phi}}$ = the variance on the average flux in the fuel,

ϕ_{ik} = the flux value measured with the fission chamber,

$\sigma_{\phi_{ik}}$ = the variance on ϕ_{ik},

V = the total volume of the fuel,

V_k = the volume of fuel effected by ϕ_{ik}

M = the number of flux measurements per vertical level.

Only eight independent flux measurements were used across the core at each vertical level in the average flux calculation and all other values of ϕ_{ik} were estimated from these eight

measurements. (See page 83) It follows then that in calculating the statistical variance on the average flux from equation (A-9) that the summation should be taken only over the number of independent measurements (i.e., k runs from k = 1 to k = 8 at each vertical level). V_k is a factor which weights the flux by the volume of the fuel estimated to produce that flux. V_k is estimated as shown in the simplified sample calculation given below.

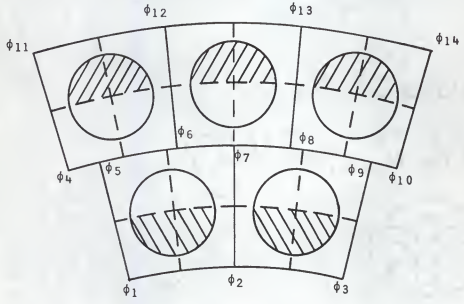

In this example ϕ_1, ϕ_4, and ϕ_{11} indicate flux values measured by the fission chamber with associated variances given by σ_{ϕ_1}, σ_{ϕ_4}, and $\sigma_{\phi_{11}}$. The average flux in the fuel elements of the sketch is calculated as discussed previously by assuming that

$$\phi_1 = \phi_2 = \phi_3,$$

$$\phi_4 = \phi_5 = \phi_6 = \phi_7 = \phi_8 = \phi_9 = \phi_{10}$$

and

$$\phi_{11} = \phi_{12} = \phi_{13} = \phi_{14}$$

Equation (A-9) for calculating the variance on $\bar{\phi}$ in this example

sums only over the three measured flux values (ϕ_1, ϕ_4, and ϕ_{11}). The volume weighting factor V_k for each of these measurements is determined by estimating a volume of fuel associated with the points at which the flux is equated to the measured flux. For example to determine V_1, the weighting factor for ϕ_1, it is assumed that ¼ of fuel element number 1 is associated with ϕ_1, that ¼ of fuel element 1 and ¼ of fuel element 2 is associated with ϕ_2, and that ¼ of fuel element 2 is associated with ϕ_3. Thus, V_1, represented by the lower cross hatched area in the sketch, is equal to the sum of these volumes or 1 volume unit, where each circular fuel element represents a unit volume. Similarly V_4, the weighting factor for ϕ_4 represented by the uncross hatched fuel elements in the center of the sketch, is equal to 2.5 volume units. V_{11}, represented by the upper cross hatched elements is equal to 1.5 volume units. Now substituting into equation (A-9) the following result is obtained

$$\sigma^2_{\bar{\phi}} = \frac{1}{25}(\sigma^2_{\phi_1} + 6.25\ \sigma^2_{\phi_4} + 2.25\ \sigma^2_{\phi_{11}}). \qquad \text{(A-10)}$$

The variance calculated from this equation is ± 5.6% of $\bar{\phi}$. Additional error in calculating the average flux in the fuel results from the uncertainty in calculating the perturbations near the control rods and the central thimble. Extensive calculations of this sort would require a large computer code and would probably not be practical on the IBM 1410 at Kansas State; therefore the approximation of equation (21) was used. Errors in calculating the flux perturbations from this expression may

be as large as ± 50%, but the effect of the local perturbations changes the total power level by an estimated ± 5%, making the uncertainty on the total power level due to local perturbation ± 2.5%. Assuming that errors due to the correction for local perturbations are independent of the statistical errors and combining these two values, the value of average flux in the fuel becomes $(1.03 \pm 0.07) \times 10^7$ n/cm^2-sec.-watt. Finally, after combining all the uncertainties the calculated power level for a power of one watt indicated by the linear recorder of the reactor console is 1.03 ± 0.11 watts.

FORTRAN Program for Calculation of the Average Flux in the Fuel

```
$JOB, POWER CALIBRATION
$COMMENT 15 MINUTES, 15 PAGES, DOUGHERTY, N. E. DEPT.
$COMMENT USES PHYSICAL TAPE 3
$ASSIGN *JR,12
$ASSIGN *G2,16
$MODE GO,TEST
$EXEC FORTRAN,,,,,,,PCALIB
      DIMENSION A(10,30),RSH(8),RP(8),RP(8),RCT(8),SUM(5)
      COMMON RLTH
    1 FORMAT(6E10.5)
    2 FORMAT(5X,13HAVERAGE FLUX=1PE14.7)
    3 FORMAT(8F10.1)
      RLTH=1.6 4853
      FLUX=0.
      Z=0.
      READ(1,3)RSH
      READ(1,3)RP
      READ(1,3)RP
      READ(1,3)RCT(1)
      DO16I=2,6
   16 RCT(I)=RCT(1)
      DO27J=1,14
      READ(1,1)A(1,1),A(2,1),A(3,1),A(4,1),A(5,1),A(6,1),A(7,1),A(8,1),A(9,1),A(10,1)
      DO6I=2,6
    6 A(I,I)=A(1,1)
      DO7I=2,6
    7 A(2,I)=A(2,1)
      DO8I=2,12
    8 A(3,I)=A(3,1)
      DO9I=2,12
    9 A(4,I)=A(4,1)
      DO10I=2,18
   10 A(5,I)=A(5,1)
      DO11I=2,18
   11 A(6,I)=A(6,1)
      DO12I=2,24
   12 A(7,I)=A(6,1)
      DO13I=2,24
   13 A(8,I)=A(8,1)
      DO14I=2,3
   14 A(9,I)=A(9,1)
      DO15I=22,27
   15 A(10,I)=A(10,21)
      READ(1,1)BR,RSH,RP
      RCT=RP
```

```
      REWIND5
      WRITE(5)(A(1,I),I=1,6),Z,Z
      CALLCORR(RCT,BCT,6)
      READ(5)(A(1,I),I=1,6)
      REWIND5
      WRITE(5)A(3,2),A(3,3),A(4,2),A(4,3),A(5,3),A(5,4),Z,Z
      CALLCORR(RSH,BSH,6)
      READ(5)A(3,2),A(3,3),A(4,2),A(4,3),A(5,3),A(5,4)
      REWIND5
      WRITE(5)A(4,6),A(4,7),A(5,9),A(5,10),A(6,9),A(6,10),A(7,12),A(7,13
     B)
      CALLCORR(RP,BP,8)
      READ(5)A(4,6),A(4,7),A(5,9),A(5,10),A(6,9),A(6,10),A(7,12),A(7,13)
      REWIND5
      WRITE(5)A(6,15),A(6,16),A(7,20),A(7,21),A(8,20),A(8,21),A(9,26),A(
     B9,27)
      CALLCORR(RR,BR,8)
      READ(5)A(6,15),A(6,16),A(7,20),A(7,21),A(8,20),A(8,21),A(9,26),A(9
     B,27)
      L=1
      M=1
      DO25K=6,24,6
      SUM(L)=(A(M,1)+A(M+1,K)+A(M,K)+A(M+1,1))/4.
      DO24I=2,K
   24 SUM(L)=SUM(L)+(A(M,I-1)+A(M,I)+A(M+1,I-1)+A(M+1,I))/4.
      L=L+1
   25 M=M+2
      SUM(2)=SUM(2)-(A(3,2)+A(3,3)+A(4,2)+A(4,3))/4.
      SUM(3)=SUM(3)-(A(5,9)+A(5,10)+A(6,9)+A(6,10))/4.
      SUM(4)=SUM(4)-(A(7,20)+A(7,21)+A(8,20)+A(8,21))/4.
      SUM(5)=-(A(9,24)+A(9,25)+A(10,24)+A(10,25))/4.
      DO26I=22,26
   26 SUM(5)=SUM(5)+(A(9,I)+A(9,I+1)+A(10,I)+A(10,I+1))/4.
      DO27N=1,5
   27 FLUX=FLUX+SUM(N)
      WRITE(3,2)FLUX
      STOP
      END
$CMS$       EXEC FORTRAN
      SUBROUTINECORR(R,B,N)
      DIMENSIONP(8),R(8)
      COMMONRLTH
      REWIND5
      READ(5)P
      REWIND5
      DO1I=1,N
      BFS=BESK( ,R(I)/RLTH)
      IF(BFS.LT.B.)BFS=1.
    1 P(I)=P(I)*(1.-B*BFS)/P(I)
      WRITE(5)P
      REWIND5
      RETURN
      END
```

```
MON#3      EXEC FORTRAN
      FUNCTION APPSER(X,N,SIGNA,I)
      IF(I.EQ.0)GO TO 2
      TERM=(4.*FLOAT(N**2)-1.)/(8.*X)
      ANPLUS=3.
      AN=2.
      GO TO 3
    2 TERM=1.
      ANPLUS=1.
      AN=1.
    3 APPSER=TERM
      AMULT=((8.*X)**2)*SIGNA
      SIGNA=4.*FLOAT(N**2)
      X=APPSER
      TERME=TERM
    4 TERM=TERM*(SIGNA-ANPLUS**2)*(SIGNA-(ANPLUS+2.)**2)/(AMULT*AN*(AN+1
     1.))
      IF(ABS(TERME).LE.ABS(TERM))GO TO 7
      APPSER=APPSER+TERM
      IF(X.EQ.APPSER)GO TO 7
      X=APPSER
      TERME=TERM
      AN=AN+2.
      ANPLUS=ANPLUS+4.
      GO TO 4
    7 RETURN
      END
MON#4      EXEC FORTRAN
      FUNCTION BESSER(N,X,SIGNA,I)
      GAMMA=.5772156649
      IF(N.NE.0)GO TO 2
      SUM=1.
      GO TO 22
    2 SUM=1./FACT(N)
      DO 21 J=1,N
   21 SUM=SUM*(X/2.)
   22 ANPLUS=N+1
      IF(I.EQ.1)GO TO 3
      VERM=ALOG(X/2.)+GAMMA
      IF(N.EQ.0)GO TO 15
      DO 12 J=1,N
   12 VERM=VERM-.5/FLOAT(J)
   15 SUM=SUM*VERM
    3 TERM=SUM
      EMULT=X*X/4.*SIGNA
      X=1.
    4 SUME=SUM
      IF(I.EQ.0)GO TO 11
      TERM=TERM/VERM
      VERM=VERM-.5/X-.5/ANPLUS
      TERM=TERM*VERM
```

```
11 TERM=TERM*FMULT/(ANPLUS*X)
   SUM=SUM+TERM
 6 ANPLUS=ANPLUS+1.
   X=X+1.
   IF(SUM.NE.SUM)GO TO 4
 7 BESSER=SUM
   RETURN
   END
$ONE$      EXEC FORTRAN
   FUNCTION BESSES(N,X,SIGNA)
   BESSES=0.
   IF(N.LE.1)GO TO 1
   DO 7 J=1,N
   MN=-N+2*(J-1)
   IF(MN.EQ.0)GO TO 4
   IF(MN.GT.0)GO TO 5
   AMULT=(2./X)**(-MN)
   GO TO 6
 4 AMULT=1.
   GO TO 6
 5 AMULT=(X/2.)**MN
 6 BESSES=BESSES+((SIGNA)**(J+1))*FACT(N-J)*AMULT/FACT(J-1)
 7 CONTINUE
 1 RETURN
   END
$ONE$      EXEC FORTRAN
   FUNCTION BESK(N,X)
10 FORMAT(1H ,27HORDER N OF BESK IS NEGATIVE)
11 FORMAT(1H ,33HARGUMENT X OF BESK IS NEGATIVE)
12 FORMAT(1H ,33HARGUMENT X OF BESK IS TOO LARGE,=,E14.6)
   PI=3.1415926535897932384626
   IF(N.GE.0)GO TO 2
   N=-N
   WRITE(3,10)
 2 IF(X.EQ.0.)GO TO 9
   IF(X.GT.0.)GO TO 4
   X=-X
   WRITE(3,11)
 4 IF(X.LT.227.5)GO TO 6
   BESK=0.
   WRITE(3,12)X
   RETURN
 6 IF(X.GE.3.3)GO TO 8
   BESK=.5*BESSES(N,X,-1.)+((-1.)**(N+1))*BESSER(N,X,1.,1)
   RETURN
 8 BESK=SQRT(PI/(2.*X))*EXP(-X)*(APPSER(X,N,1.,0)+APPSER(X,N,1.,1))
   RETURN
 9 BESK=.99999999999999E+99
   RETURN
   END
```

```
$RUN$$      EXEC FORTRAN
  FUNCTION FACT(N)
7 FORMAT(1H ,3 ARGUMENT FOR FACT IS TOO LARGE)
  FACT=1.
  IF(N)1,2,4
1 FACT=.99999999*.99999999E38
  IF(N-(N/2)*2)2,3,2
3 FACT=-FACT
  RETURN
4 DO 5 I=1,N
  FACT=FACT*FLOAT(I)
  CALL OVERFL(J)
  IF(J.EQ.1)GO TO 6
5 CONTINUE
2 RETURN
6 WRITE(3,7)
  RETURN
  END
$CONTROL    EXEC LINKLOAD
            CALL PCALLS
$CONTROL    EXEC PCALLS,MJC
```

NOMENCLATURE

A	activity, (dis./sec.)
A_b	activity of a bare foil
A_{cd}	activity of a cadmium covered foil
A_p	atomic weight of phosphorous
A_s	atomic weight of sulfur
A_o	zero time activity
A_1	area under photopeak #1
A_2	area under photopeak #2
A_{12}	area under the sum peak
A_{235}	atomic weight of U-235
B	experimentally determined proportionality constant for the effects of a control rod on the neutron flux
C	count rate
C_p	initial saturated count rate from the phosphorous pellet
C_s	initial saturated count rate from the sulfur pellet
C_o	zero time count rate
E	energy
e_1 & e_2	probabilities that gamma 1 and gamma 2 are absorbed in the crystal by a photoelectric process
F_{cd}	correction for epithermal absorption of neutrons in cadmium
F_{th}	correction for flux depression in the vincinity of a foil
K	energy released per fission
K_s	isotopic content of S^{32}
$K_o(\kappa r)$	zero order modified Bessel function of the second kind

m	mass
N_a	Avogadro's number
n	total neutron density, (n/cm^3)
n_b	the background coincidence count rate
n_r	random coincidence count rate
n_β	count rate from the beta detector
n_γ	count rate from the gamma detector
$n_{\beta\gamma}$	beta-gamma coincidence count rate
$n^*_{\beta\gamma}$	total observed beta-gamma coincidence count rate
P	power
R	cadmium ratio
r	radial distance
S_p	content of P^{32} in the phosphorous pellet in weight percent
T	total area under the gamma spectrum
t	time
t_1 & t_2	probabilities that gamma 1 and gamma 2 are absorbed in the crystal by any means
V	volume
V_c	volume of the fuel in the core
$\bar{v}$	mean velocity of neutrons in the reactor core
v_o	most probable neutron speed in a Maxwellian distribution at 293^o K
α	ratio of the resonance component of the resonance activation to the 1/v component
δ_i	least squares error associated with the i^{th} count rate
ϵ_β & ϵ_γ	efficiencies of the beta and gamma detectors respectively

κ	$1/L_{th}$, where L_{th} is the thermal diffusion length
λ	radioactive decay constant
Σ_a	macroscopic absorption cross section
Σ_f	macroscopic fission cross section
σ_A	standard deviation on activity A
σ_{C_o}	standard deviation on the count rate C_o
$\sigma(E)$	microscopic activation cross section as a function of energy
σ_f	microscopic fission cross section
σ_i	standard deviation on the i^{th} count rate
σ_p	microscopic cross section for P^{31}
$\int \sigma_r dE/E$	resonance portion of the total resonance activation integral
$\int \sigma_{1/v} dE/E$	1/v portion of the total resonance activation integral
σ_o	saturation cross section for the $S^{32}(n,p)P^{32}$ reaction
σ_ϕ	standard deviation on the flux ϕ
τ	resolving time of the coincidence circuit
ϕ	neutron flux, $(n/cm^2\text{-sec})$
ϕ_f	integrated fast flux above 2.9 Mev
ϕ_r	resonance neutron flux
ϕ_{th}	thermal neutron flux

EXPERIMENTAL NEUTRON FLUX MEASUREMENTS AND POWER CALIBRATION IN THE KANSAS STATE UNIVERSITY TRIGA MARK II NUCLEAR REACTOR

by

GARY DON BOUCHEY

B. S., Kansas State University, 1966

AN ABSTRACT OF A MASTER'S THESIS

submitted in partial fulfillment of the

requirements for the degree

MASTER OF SCIENCE

Department of Nuclear Engineering

KANSAS STATE UNIVERSITY
Manhattan, Kansas

1967

Approved by:

Major Professor

The purpose of this work is to determine experimentally the neutron flux in the Kansas State University TRIGA Mark II nuclear reactor and to use the measured flux to calculate the power generated by the reactor. "Westcott convention" was used throughout this work for reporting neutron flux because of the convenience of this definition for experiments involving the calculation of reaction rates. Absolute thermal neutron flux is measured at a selected position in the thermal column and used as a standard for calibration of all other flux measurements. The calibration point in the thermal column also provides a known thermal flux which may be useful for many experiments at Kansas State. Thermal, resonance, and fast fluxes are measured at the point of maximum flux in the central thimble and in the rotary specimen rack. Vertical plots of thermal flux are obtained with a miniature fission chamber inserted into the reactor core through the foil insertion holes in the top grid plate. By numerical integration of the thermal flux data obtained with the fission chamber, the average flux and the corresponding power output of the core are calculated. At an indicated power level of one watt on the reactor console, the power calculated from the flux data was 1.03 ± 0.11 watts.